Palaeontologia Electronica
palaeo-electronica.org

A new multi-faceted framework for deciphering diplodocid ontogeny

D. Cary Woodruff, Denver W. Fowler, and John R. Horner

ABSTRACT

Determining maturity in sauropod dinosaurs histologically is problematic as rapid growth leads to remodeling of Lines of Arrested Growth (LAGs). Although a complimentary system has been devised utilizing several factors including relative amounts of remodeling (Histologic Ontogenetic Stage [HOS]), most assessments of sauropod maturity are based on morphologic indicators. To better assess skeletal maturity and morphologic change through ontogeny, we examined cranial and postcranial material from over 20 diplodocid individuals (*Apatosaurus* and *Diplodocus*) from the Upper Jurassic Morrison Formation. Here we describe consistent combinations of morphologic and histologic features that can be used to ascertain maturity. Small diplodocids (femoral lengths ≤120 cm) display non- to weakly bifurcated cervical and dorsal neural spines, acamerate to camerate centra, two to six preserved LAGs in dorsal ribs, and a maximum femoral designation of HOS 7. Larger individuals (femoral length ~125 cm) have more developed internal pneumatic structures, greater neural spine bifurcation, preserve up to eight LAGs, and a femoral designation of HOS 9. In contrast, skeletally mature sauropods (femoral lengths >150 cm) have complex pneumatic structures, extended neural spine bifurcation (also within anterior caudals), and a femoral HOS between 11-13. Further, all of the preserved small diplodocid skulls exhibit a postparietal foramen (previously suggested to be an apomorphy of Dicraeosauridae), which is absent in large skulls (where preserved), suggesting that it is an ontogenetic character. These findings support the hypothesis of significant ontogenetic morphological change in diplodocid sauropods and suggest caution when describing new taxa on the basis of small-bodied holotypes.

D. Cary Woodruff. Royal Ontario Museum; University of Toronto, Toronto, ON, Canada; and Great Plains Dinosaur Museum and Field Station, Malta, MT, United States of America. sauropod4@gmail.com
Denver W. Fowler. Dickinson Museum Center, Dickinson, ND, United States of America. df9465@hotmail.com
John R. Horner. Burke Museum of Natural History and Culture, University of Washington, Seattle, WA, United States of America. johnrhorner@mac.com

Woodruff, D. Cary, Fowler, Denver W., and Horner, John R. 2017. A new multi-faceted framework for deciphering diplodocid ontogeny. *Palaeontologia Electronica* 20.3.43A: 1-53
palaeo-electronica.org/content/2017/1918-deciphering-diplodocid-growth

Keywords: diplodocid; ontogeny; morphology; histology

Submission: 20 April 2016 Acceptance: 19 June 2017

INTRODUCTION

Studies of ontogenetic morphological change in dinosaurs largely rely on comparisons of cranial features (i.e., horns, frills, and crests; Dodson, 1975; Hopson, 1975; Sampson et al., 1997; Carr, 1999; Evans et al., 2005; Horner and Goodwin, 2006; 2009; Scannella and Horner, 2010; Campione and Evans, 2011). As cranial material of sauropods is relatively rare and does not exhibit pronounced display structures (which are often beneficial in recognizing ontogenetic trajectories [e.g., Dodson, 1975]) the work done on them has to depend largely on histology. These histologic studies examine the microstructure of the bone and the degrees of bone remodeling to determine relative maturity of a range of individuals, such as the Age Class assignments of Curry (1999) and the Histologic Ontogenetic Stage (HOS) of Klein and Sander (2008). Yet while the particulars and demarcations of these maturational assessments may vary, all acknowledge that histologically, skeletal maturity occurs at the onset of an external fundamental system (EFS; slowly deposited parallel-fibered or lamellar tissue along the outermost cortex - closely spaced outermost series of LAGs [Huttenlocker et al., 2013; Appendix 1]), which is the histologic indicator of osteogenic cessation (see Padian and Lamm [2013] for a greater discussion of bone tissues throughout maturity).

Recently several sauropod studies have reported morphologic attributes that can be used to denote maturity. Whitlock et al. (2010) documented cranial changes between immature and mature specimens of *Diplodocus* (or Diplodocinae indeterminate [Tschopp et al., 2015]), which include the development of proportionally larger orbits, rounded and narrower premaxilla, and a more anteriorly situated tooth row. Wedel (2003, 2005, 2009), Schwarz et al. (2007a), and Carballido and Sander (2014) have demonstrated that the complexity of pneumatic architecture has increased through sauropodomorph phylogeny and likewise increased through ontogeny. Salgado (1999) suggested a link between the degree of neural spine bifurcation and ontogeny in diplodocids. Woodruff and Fowler (2012) showed that small (presumably immature) diplodocids exhibited rounded to weakly bifurcated neural spines, whereas neural spines were fully bifurcated in larger (and presumably more mature) individuals. Based on this observation, it was suggested that the degree of bifurcation could be used to infer maturity in diplodocids (and other methodologies have used morphology to predict maturity; such as the Morphologic Ontogenetic Stage [MOS] of Carballido and Sander, 2014; or the ontogenetic trajectory stages of Ikejiri et al., 2005).

While some of these morphologic features have been incorporated into our understanding of sauropod ontogeny, the conclusions of Woodruff and Fowler (2012) have been the subject of ongoing discussion (Wedel and Taylor, 2013; Carballido and Sander, 2014; Hedrick et al., 2014; Woodruff and Foster, 2014; Tschopp et al., 2015). Aspects of this study that are considered contentious include: 1) the unknown precise serial placement for isolated vertebrae, and 2) the proper identification of maturational states to corroborate said morphological interpretations (Wedel and Taylor, 2013; Hedrick et al., 2014). While these are issues that need to be further addressed through continued morphological studies of sauropod growth, it has been suggested that histologic analysis may not be necessary due to specific features attributable to maturity (such as vertebral arch fusion; Wedel and Taylor, 2013). We would argue that histologic analysis is the only repeatedly confirmed methodology to determine a specimen's maturational state. The current analysis tests the inferred maturational stages of Woodruff and Fowler (2012) using histologic examination. Additional features that may indicate relative maturity are also assessed. A multi-faceted approach, incorporating examination of overall vertebral morphology (cervical, dorsal, and anterior caudal vertebrae), vertebral pneumatic morphology, histologic ontogenetic stage (HOS; Klein and Sander, 2008), histologic and morphologic examination of femora, age determining histology of dorsal ribs, and neural spine histology (of cervical and dorsal vertebrae) was conducted on various members of Diplodocoidea, with primary emphasis on *Apatosaurus* and *Diplodocus* (Appendix 2).

MATERIALS AND METHODS

Institutional Abbreviations

All of the specimens examined in this analysis are housed in recognized repositories and are freely available for study by qualified researchers. Repositories in this analysis are as follows: Academy of Natural Sciences of Drexel University, ANS; American Museum of Natural History, AMNH; Carnegie Museum of Natural History, CM; Brigham Young University, BYU; Cincinnati Museum Center, CMC; Dinosaur National Monument, DNM; Houston Museum of Natural Science, HMNS; Great Plains Dinosaur Museum, GPDM; Museum of the Rockies, MOR; Museum of Western Colorado, MWC; National Museum of Nature and Science, NSMT; Sam Nobel Oklahoma Museum of Natural History, OMNH; Sauriermuseum Aathal, SMA; Science Museum of Minnesota, SMM; Texas Memorial Museum, TMM; United States National Museum, USNM; University of Kansas Natural History Museum, KUVP; Yale Peabody Museum, YPM.

Taxonomy and Terminology

The sauropods examined in this analysis all come from the Upper Jurassic Morrison Formation of North America. While numerous genera of Diplodocoidea and even Macronaria were examined, the presented analysis will attempt to restrict a majority of the results and discussion to the Diplodocidea *Apatosaurus* and *Diplodocus*. While many maturational hierarchies for sauropods (e.g., Curry, 1999; Ikejiri et al., 2005; Klein and Sander, 2008; Carbadillo and Sander, 2014) and other dinosaurs (Hone et al., 2016) exist, we refrained from initially using such divisions to avoid introducing preconceived ontogenetic hypotheses (i.e., not assigning maturity of a specimen before the analysis). While elemental and body size generally correlates with age – and we were tempted to colloquially refer to small individuals as “younger”, and vice versa – a whole suite of variables (including intraspecific variation) could be concealed by such basic assumptions. Throughout this analysis, for each feature examined the smaller (and presumably more immature) specimens are described first, progressing to larger (presumably more mature).

Histological descriptions follow those established by Francillon-Vieillot et al. (1990), de Ricqlès et al. (1991), Castanet et al. (1992), and Huttenlocker et al. (2013), while long bone descriptions follow the HOS of Klein and Sander (2008; histological terminology can be found in Appendix 1). Throughout this study the terms “immature” and “mature” are used to refer specifically to skeletal maturity (mature = the presence of an external fundamental system [EFS], immature = lacks an EFS). Of interest, it is important to note the extensive colloquial and defined usages of “immature” and “mature”. Although such informal maturational phrasing can be convenient, with the pervasive usage and varying connotations applied to such terms, definition methodology must be strictly followed (for a good explanation of this situation, see Hone et al. [2016]).

One vertebral feature examined in this analysis is the bifurcated neural spine. Consisting of a paired neural spine (which can be expressed within the cervical, dorsal, and caudal series), bifurcated neural spines are found in several sauropodomorph clades and families, including: Vulcanodontidae, Mamenchisauridae, Diplodocoidea, Camarasauridae, Brachiosauridae, Turiasauria, and Titanosauria (Woodruff, 2016). Throughout this analysis, the term bifurcation shall initially follow that of Janensch’s (1929) definition to indicate a paired neural spine. While the ontogenetic development of this feature is still under study (see Woodruff and Fowler, 2012 and Wedel and Taylor, 2013), Wedel and Taylor (2013) categorized spine apex states and the degrees of bifurcation – 1) unsplit, 2) notched, 3) shallowly bifid, 4) deeply bifid. If bifurcation does develop ontogenetically, then the spine apex would progress from unsplit to bifid. In this analysis we shall follow that any unsplit or rounded spine apex is indeed not bifurcated, while any spine apex that ranges from notched to any degree of bifid is categorized herein as bifurcated.

A recent analysis of Diplodocidea (Tschopp et al., 2015) suggests that this group may be more speciose than previously thought. We will follow the taxonomy of this study and use the multi-faceted approach to determining sauropod ontogeny to examine growth and variation in this group in order to review the proposed distinction of these taxa.

Histologic Methodology

Sauropod elements were photographed from multiple angles (if possible), and all measurements were taken with digital calipers and cloth or retracting measuring tapes. For histological sampling, sites were chosen as follows (Figure 1): for dorsal ribs, sections were removed just distal to the capitulum and tuberculum (following the methods of

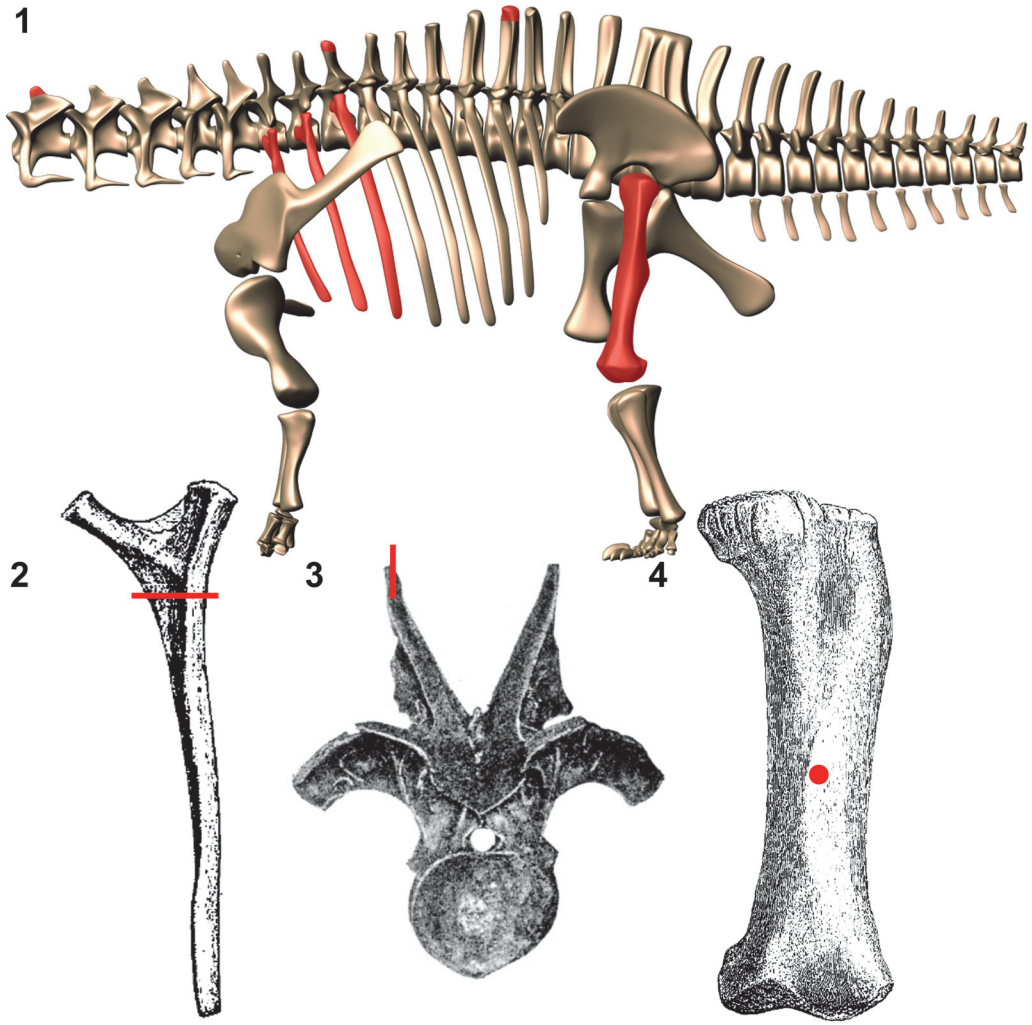

FIGURE 1. Elements histologically sampled for this analysis. **1,** Digital reconstruction of *Apatosaurus louisae* (by K. Stevens) with sampled elements highlighted in red. Approximate location of sampling in dorsal ribs (**2**; from Gilmore, 1936), neural spines (**3**; from Hatcher, 1901), and femora (**4**; from Gilmore, 1936).

Waskow and Sander, 2014). If a specimen was small enough, entire transverse sections of the dorsal ribs were taken, while from larger specimens a medial section was removed distal to the capitulum and tuberculum. For limb elements (femora), core sections were removed from the anterior face of the middle of the diaphysis. A longitudinal orientation line was drawn on the periosteal surface, and thin sections were taken perpendicular to this line (Stein and Sander, 2009). If a core broke during drilling, the fragments were pieced back together to the extent that was possible in order to examine microstructure.

For samples in this analysis, previously occurring cracks and fractures were exploited if possible. A section of bone containing the desired sample location that had been glued together could be removed (by application of heat or a solvent), from which the section could be molded and cast. If previously occurring fractures could not be exploited, either a rotary tool (Dremel™) with a 3.8 cm diamond cutting wheel or a 10.8 cm diamond bladed tile saw (WorkForce™) were used to make two parallel incisions. However, no bone was cut in its entirety to remove sample material. The bone that is lost due to the cutting blade (called kerf loss) results in adjoining flush edges. During restoration work, these flush edges can result in the element having a different measurement (usually shorter, and depending on the blade width this could be the greater part of a cm discrepancy). When cutting an element, the incisions were made only partially through the bone. From here the desired sample section could be broken out, which produces a

jointed edge, allowing for a precise connection for the casted section.

The coring bits pioneered by Sander (1999; 2000) and Stein and Sander (2009) allow for removal of a cylindrical sample of bone, and this can be performed in a variety of locations (such as a collection room, a lab, and even on a mounted specimen). These bits are cylindrical tools consisting of a flat end with sintered or galvanized diamond grit. In our sampling we observed that these flat end bits created a significant degree of friction and often caused flaking or chipping of the periosteal surface. Instead, damage to the periosteal surface was negligible with a serrated core bit. In like manner when sawing across wood grain, sheet woods, or delicate materials such as plexiglass, the presence of smaller and finer blade teeth in tandem produce a smoother cut. In addition to the serrated tip, we found a bit that separated into two sections (known as a two-part bit) to be invaluable. With a traditional bit, the core can become lodged and extremely difficult to remove, and attempted removal can damage or destroy the bone core. However, using a 35 mm two-part bit (Bosch™) allows for a coin (under 35 mm in diameter) to be placed on the bone surface without interfering with the cutting surface. If the core becomes lodged in the bit, the bit can simply be separated, and a larger diameter bolt (such as a carriage bolt) can be inserted into the distal half and used to indirectly push on the bone core via the coin (opposed to direct pressure on the bone surface, which could cause damage; Figure 2).

In addition to the information pertaining to the core bit itself, we found other useful techniques to aid in the coring process. In the case of a delicate periosteal surface, a thick layer of fossil preservative (such as Vinac/McGean B-15) can be applied to the selected surface. Once dry, a layer of five-minute epoxy resin can be placed on top of the thick preservative layer, which prevents external flaking, and subsequently cored through. Afterwards acetone can be used to clean the area surrounding the bore hole, and the surface of the core if desired. Regarding use of the lubricant, Stein and Sander (2009) suggest making a clay reservoir around the core to contain the lubricant (in most cases water). This keeps the mess to a minimum, but using a squirt bottle to apply a soap and water solution to the bit during coring provides the same effect. The water cools the bit, while the soap provides extra lubrication. It is best to apply frequent lubrication, and always avoid dry bone dust for health and safety reasons, especially with potentially radioactive fossils.

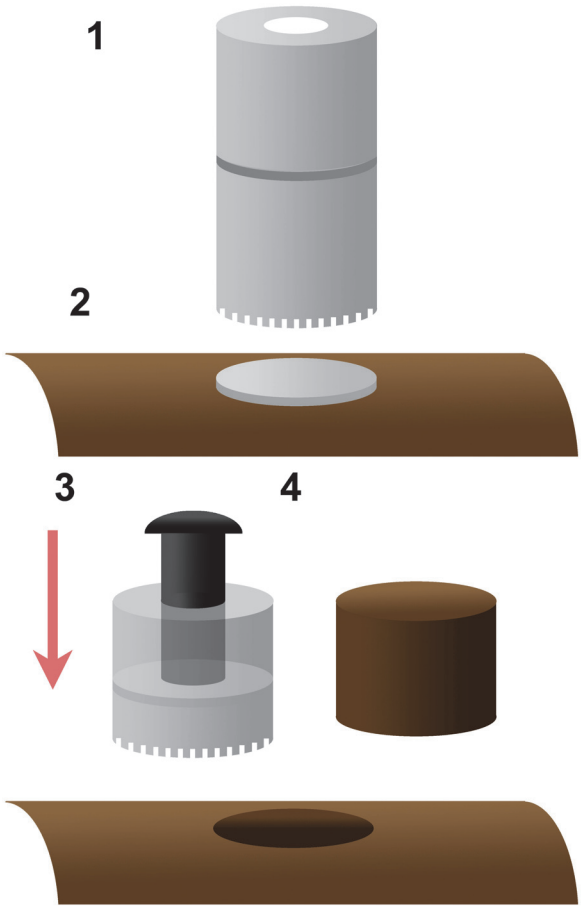

FIGURE 2. Schematic of coring bit method used in this analysis**.** A two part Bosch™ core bit (**1**) with a coin placed on the bone surface prior to coring (**2**), the core bit separated post coring, with a bolt inserted to push on the coin (**3**) to extract the bone core (**4**).

In the case of a delicate cortex, a stepwise progression is best: core a short distance into the bone (a few mm), extract the bit, and inject some form of penetrating glue into the scored area. Heating the bone with a blow dryer (standard handheld hair dryer) prior to the introduction of glue will aid the bone in absorbing the glue. Allowing for ample drying time (several hours) is imperative; otherwise the bit can become gummed up and will be more susceptible to catching. If the bit and core do become gummed up or glued together, soaking the bit in a cup filled with an adhesive remover (such as *CYANO*-OFF!™) overnight will dissolve the glue. Doing this stepwise progression will stabilize both the core and surrounding area.

All samples used for histological analysis were prepared following the methods and techniques demonstrated in Padian and Lamm (2013). Samples were first embedded in a Silmar two-part epoxy resin (SIL95BA-41), and once cured, two transverse slices (~2-4 mm thick) were cut from the embedded block using a Felker 41-AR tile saw. Slices were then pre-mount ground on the surface to be glued to the glass slide using 320 grit and then 600 grit silicon carbide paper. After this initial grinding, the sample is mounted to frosted glass slides using a Devcon two-part epoxy glue. Then using a Buehler Ecomet 4 Variable Speed Grinder-Polisher, the thin sections were polished using Buehler silicon carbide paper sequentially from a 60 grit to an 800 grit finish. Final slide thickness was approximately ~150 µm, but varied between samples to achieve similar optical clarity. Finished slides were photographed using a Nikon Optiphot-Pol polarizing microscope equipped with a Nikon DS-Fi1 digital camera and compiled with NIS-Elements BR 3.0 software.

In addition to the histologic analyses, Computed Tomography scans (CT scan) of cervical and dorsal vertebrae were performed to examine pneumatic architecture. CT scanning was conducted by Advanced Medical Imaging at Bozeman Deaconess Hospital in Bozeman, MT, U.S.A. using a Toshiba Aquilion 64 CT Scanner. The peak kilovoltage (pKv) for each scan was approximately 135 pKv, and scan resolution (varied due to the dimensions of each vertebra) ranged from every 2 mm up to 5 mm. Scan data were uploaded into the DICOM Viewer OsiriX for multi-plane study, with individual planes being analyzed using the image processing program ImageJ (Abramoff et al., 2004).

Examination Methodology

In exceptional ontogenetic studies, large sample sizes including representatives of multiple growth stages allow for more comprehensive histologic and morphological comparisons (e.g., Dodson, 1975; Carr, 1999; Scannella and Horner, 2010; Horner et al., 2011; Frederickson and Tumarkin-Deratzian, 2014; Woodward et al., 2015). While Morrison diplodocids are by far one of the most common of all North American dinosaur groups, taphonomic biases, stratigraphic resolution, and taxonomic uncertainties generally result in largely incomplete and less well understood individuals.

Several studies have previously documented possible ontogenetic changes in sauropods (including pneumatic architecture, Wedel [2003]; HOS, Klein and Sander [2008]; cranial changes Whitlock et al. [2010]; neural spine bifurcation, Woodruff and Fowler [2012]; MOS, Carballido and Sander [2014]; LAG record, Waskow and Sander [2014]); yet the majority of these analyses examine a single feature (e.g., spine bifurcation [Woodruff and Fowler, 2012]) or a single methodology (i.e., morphology or histology; HOS [Klein and Sander, 2008]). While all of these previous works are invaluable contributions to our understanding of sauropodomorph paleobiology, they represent individual puzzle pieces. Although beneficial, such analyses have little capacity to reflect on the individual sauropod as a whole. Since there are differences in histologic, morphologic, or cladistic approaches, different emphases may lead to conflicting taxonomic interpretations (as in the case of *Suuwassea* or SMA 0009; Harris [2006a]; Schwarz et al. [2007b]; Whitlock and Harris [2010], Carballido et al. [2012]; Woodruff and Fowler [2012]; Tschopp et al. [2015]).

However, by analyzing a range of skeletal features, and including varied histologic and morphologic examinations, such an encompassing methodology can allow for better resolution of the entire animal. In lieu of a much larger sample of complete diplodocid specimens forming an ontogenetic series, the available material has been used to build an encompassing set of histologic and morphologic features creating a system of supportive characters that we term the Histo-Morph Ontogeny Scale (H-MOS; Appendix 3).

Methodology of Examined Skeletal Features

CT scans of pneumatic architecture. The hypothesis that vertebral pneumatic architecture develops ontogenetically is strongly supported (Wedel, 2003), but has yet to be documented both externally and internally within an ontogenetic series (note Carballido and Sander [2014] do demonstrate external pneumatic architecture among ontogenetic stages of *Europasaurus*). In order to document this pattern within an ontogenetic series, we examined the internal morphology of cervical and dorsal pneumatic structures from our ontogenetic series using Computed Tomography (CT scan). Only cervical and dorsal vertebrae from known or confidently estimated positions were scanned. The scanned elements consist of two anterior to middle cervical vertebrae from two individuals (MOR 714 [diplodocid indeterminate] and MOR 790 [*Diplodocus* sp.]), two anterior dorsal vertebrae from two individuals (MOR 790 and MOR 592; both *Diplodocus* sp.), and three poste-

rior dorsal vertebrae from three individuals (MOR 790, MOR 592 [both *Diplodocus* sp.], and MOR 957 [*Apatosaurus* sp.]). Each specimen was examined via frontal and transverse sections. Definitions and usage of pneumatic architecture follow those established by Wedel et al. (2000; Appendix 1).

Vertebral neural spines. To determine if morphological changes in neural spines correspond with changes in microstructure, four neural spine apices (two posterior cervical vertebrae [MOR-790 unnumbered and MOR 592 8-24-90-91; both *Diplodocus* sp.] and two anterior dorsal vertebrae [MOR 790 8-21-95-238 and MOR 592 8-22-90-15; both *Diplodocus* sp.]) were coronally sampled to examine histology across the neural spine, and between varying body sizes.

Dorsal ribs. Because sauropods grew so rapidly and their limb bones were generally highly remodeled, lines of arrested growth (LAGs) in limbs are not well preserved, making age determination difficult. Due to the challenges involved with sauropod limb histology, Waskow and Sander (2014) and Waskow and Mateus (2017) recently demonstrated that dorsal ribs record cyclical growth marks. The identification and recognition of recordable growth histories in sauropods finally allows for histological age determination (opposed to maturational inference [HOS] and tabulated longevity calculations). Waskow and Sander (2014) found that sampling dorsal ribs 1-3 within the proximal third of the rib, but distal to the capitulum and tuberculum, recorded the most intact and complete history of growth marks (LAGs).

In this analysis, we sampled the dorsal ribs of four diplodocids (MOR 790 7-24-96-95, MOR 790 7-27-8-96, MOR 592 [all *Diplodocus* sp.], CM 94 [*D. carnegii]*). Unfortunately no articulated *Apatosaurus* or *Diplodocus* dorsal rib cages were available for this analysis; therefore specimens could only be selected by size and thus hypothesized maturity (smaller - presumably less mature, larger - presumably more mature). For these isolated ribs, individual morphology was heavily scrutinized in order to make sure serial positions were consistent. Further, following Waskow and Sander (2014), we examined the histology of femora associated with the sampled dorsal ribs (note that MOR 592 [*Diplodocus* sp.] is the only specimen that is represented by a single individual; MOR 790 [*Diplodocus* sp.] comes from a bone bed which consists of an MNI of 15 [Storrs et al., 2012], and CM 94 [*D. carnegii*] of an MNI of 2 [Hatcher, 1901]). See sections discussing MOR 790 for how we selected elements/individuals). For isolated dorsal ribs, comparisons to well-documented rib series were used to approximate serial position (*Dicraeosaurus* – Janensch, 1929; *Apatosaurus* – Gilmore, 1936).

For *Apatosaurus* and *Diplodocus* in this dataset, estimated individual age was based on preserved LAG counts. From the preserved LAG record, Griebeler et al. (2013) and Waskow and Sander (2014) use a retro-calculation method to formulate age estimates. For the retro-calculation, the minimum and maximum distance between LAGs must be measured. Lines are then drawn along the short and long axis, with the origin representing the hypothetical original center of the rib. From there the previously measured distances are marked until reaching the origin and thus attaining a hypothetical maximum age value. While this methodology is convenient, straightforward, and simplistic, this retro-calculation method implies uniform growth rates throughout ontogeny. Whereas some studies suggest that sauropods had a slower initial growth rate (e.g., Erickson et al., 2001; Rogers and Erickson, 2005; Griebeler et al., 2013), others indicate that immature dinosaurs exhibited faster growth early in ontogeny (Curry, 1999; Horner et al., 1999, 2000; Sander, 2000; Erickson et al., 2001; Padian et al., 2001; Horner and Padian, 2004; Sander et al., 2004; Erickson, 2005; Lee and Werning, 2008; Lehman and Woodward, 2008; Woodward and Lehman, 2009; Sander and Tückmantel, 2003; Fowler et al., 2011; Tsuihiji et al., 2011; Campione et al., 2013). If so, the distances between LAGs in immature diplodocids should be greater during early development. Thus the retro-calculation methods likely represent maximum age estimates. However, this retro-calculation method will be beneficial in the analysis of specimens with significantly more remodeling in which LAG counts are obscured and thus maximum age can be estimated.

Femora. To analyze relative maturities using long-bone histology, this analysis relied heavily on the sample set and HOS of Klein and Sander (2008). Two femora from this study's dataset were sectioned (MOR 790 and MOR 592 [both *Diplodocus* sp.]) and compared to the Klein and Sander (2008) samples to support previously inferred and hypothesized maturational stages. Histological designations for femora in this analysis follow the numerical and alphabetical designations of Klein and Sander (2008). The histological ontogenetic stage (HOS) of Klein and Sander (2008) follows a 13-part maturational system – HOS 1 being the most immature bone tissue types, HOS 13 the old-

est – which consists of a 7-part alphabetical hierarchy denoting bone microstructure – bone Type A having no primary osteons, bone Type G consisting entirely of multi-generational secondary osteons (Klein and Sander, 2008). However, in any analysis using the HOS, one must be aware that HOS values do not correspond to age of the individual; e.g., an HOS of 4 does not correspond to a four year old animal – it represents a demarcated designation in bone tissue morphology.

Body mass estimates were calculated for fifty-four diplodocid femora (Appendix 4) following the allometry-based body mass formula of Mazzetta et al. (2004). Additional mass estimation methods that incorporate multiple elements (such as humeral and femoral circumference; i.e., Campione and Evans, 2012) and histologic data (Sander and Tückmantel, 2003; Lehman and Woodward, 2008; Griebeler et al., 2013) should produce more accurate estimates because these methods incorporate more variables regarding the individual and its life history. However, the diplodocid dataset in this analysis lacks the required inclusive life history variables (i.e., corresponding femur and humerus [Campione and Evans, 2012], or histologic markers - LAGs or polish lines [Sander and Tückmantel, 2003; Griebeler et al., 2013]). As such the most agreeable method that can be incorporated with this dataset is that of Mazzetta et al. (2004). Once mass values were calculated, 10% was deducted to account for pneumaticity (following Wedel, 2003). Since the degree of pneumatization at different body sizes is not known, we decided to deduct a standard value of pneumatization. However, it is important to note that such standardization would imply isometry, which this analysis clearly advocates against; therefore 10% reduction could represent the maximum for immature and the minimum for mature animals.

RESULTS

Morphologic Data

Neural spine bifurcation. As stated previously, one of the two contentious points to the Woodruff and Fowler (2012) findings is whether neural spine bifurcation follows an ontogenetic trajectory (Wedel and Taylor, 2013). Much of this disagreement arises from the use of isolated elements where precise serial placement is at best an approximation (such as the material from the Mother's Day Quarry); and we agree that serial position is important in regards to spine bifurcation.

It is unequivocal that the degrees and morphology expressed in neural spine bifurcation vary amongst all of sauropods with this vertebral modification (*sensu* Woodruff, 2016). Likewise the complex relationship between vertebral column length, column mass, column mobility, and size of the individual animal are all factors that affect and influence bifurcation, even within the same taxon (Woodruff, 2016; Woodruff and Foster, 2017). Therefore we should not think of bifurcation as a static developmental process, and we now know this "defined" pathway as originally proposed by Woodruff and Fowler (2012) is not an entirely accurate reflection. Amongst certain taxa spine bifurcation may progress from rounded to fully bifid in one, notched to shallowly bifid in another, or shallowly to fully bifid in a third. While the initial and final spine condition may vary across taxa - and certainly the mechanics of the cervical columns do vary across taxa – spine morphologies do vary in some capacity from immature to mature individuals. While some of these developmental trajectories may be more dramatic than others (*Diplodocus* [Woodruff and Fowler, 2012] compared to *Barosaurus* [Melstrom et al., 2016]), any morphologic change through growth is ontogenetic development in any definition or capacity. Since Woodruff and Fowler's (2012) initial report, the authors have examined material representing a significant portion of known Morrison diplodocids collected to date (and ongoing work by DCW). In addition to the numerous isolated elements, enough associated, formerly articulated, and articulated specimens demonstrate that while there is a great degree in variation in every respect, neural spine bifurcation does indeed develop ontogenetically (Figure 3).

Postparietal foramen. In some sauropods, there is a cranial foramen situated between the posterior portion of the parietals and the anterior portion of the supraoccipital. Known as the postparietal foramen, this feature has been inferred as a synapomorphy of Dicraeosauridae (Salgado and Bonaparte, 1991; Harris, 2006a; Remes, 2009; Whitlock, 2011a), an autapomorphy for the plateosaurian sauropodomorphs *Massospondylus* and *Plateosaurus* (Knoll et al., 2012), the basal sauropod *Spinophorosaurus* (Knoll et al., 2012), and the diplodocids *Tornieria* (Upchurch et al., 2004a; Remes, 2009), *Kaatedocus* (Tschopp and Mateus, 2013), and *Galeamopus* (Tschopp et al., 2015). Yet outside of *Kaatedocus, Galeamopus, Tornieria,* and *Suuwassea* (Lovelace et al., 2007; Whitlock and Harris, 2010; Whitlock, 2011a; Woodruff and Fowler, 2012), no members of Diplodocidae or

FIGURE 3. Ontogenetic development of neural spine bifurcation in Morrison Formation sauropods. Apatosaurinae – represented by the immature individuals CM 555 (*Apatosaurus excelsus* or *Brontosaurus excelsus*) and CM 3390 (*Apatosaurus* sp.) compared to the mature 3018. *Diplodocus* – represented by the immature MOR 592 (*Diplodocus* sp.) compared to the mature CM 84 (*Diplodocus carnegii*). *Camarasaurus* – represented by the immature CM 11338 (*Camarasaurus lentus*) compared to the mature AMNH 5761 (*Camarasaurus supremus*). *Barosaurus* – represented by the immature AMNH 7535 compared to the mature AMNH 6341. Images not to scale. Scale bars equal 10 cm.

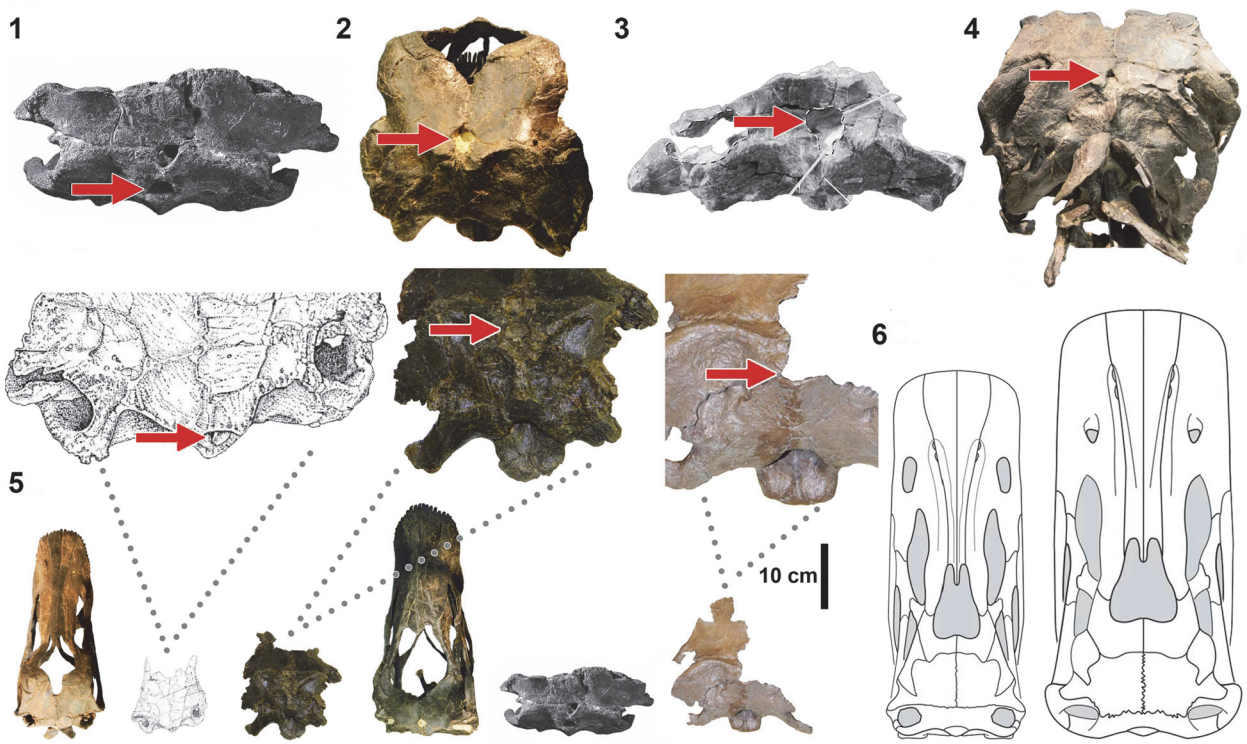

FIGURE 4. Presence of the Postparietal Aperture within Diplodocidea (indicated by red arrows). **1-4,** Diplodocid specimens with the Postparietal Aperture: **1,** *Suuwassea* (ANS 21122); **2,** *Galeamopus* (SMA 0011); **3,** *Apatosaurus* sp. (BYU 17096) (Balanoff, et al., 2010); **4,** *Kaatedocus* (SMA 0004). Note **1** and **3** are dorsal views while **2** and **4** are posterior views. **5-6,** Diplodocid skulls illustrating the presence of the Postparietal Aperture in immature individuals (**5**-image courtesy of the Science Museum of Minnesota), and its absence in mature individuals (**6**). For **5**, from left to right: *Kaatedocus* (SMA 0004), *Diplodocus* sp. (SMM P. 84.15.3), *Apatosaurus* sp. (MOR 700), *Galeamopus* (SMA 0011; this skull is partially damaged, so the morphology of the foramen may be distorted), *Suuwassea* (ANS 21122), and *Diplodocus* sp. (MOR 592). For **6**, note that the *Diplodocus* and *Apatosaurus* skulls are stylized renderings based on multiple specimens (from Whitlock [2011b]; *Diplodocus* sp. to scale of USNM 2672, and *Apatosaurus louisae* to CM 11162). Skulls in **5** and **6** to scale.

other Late Jurassic sauropods are known to possess this cranial feature; however, given the scarcity of sauropod cranial material, it is possible that this feature may be more widespread in Sauropoda (Harris, 2006a; Whitlock and Harris, 2010; Hedrick et al., 2014).

Balanoff et al. (2010) reported an *Apatosaurus* sp. braincase (BYU 17096) with a postparietal foramen, making it the first definitive member of Apatosaurinae to possess this feature. Subsequent examinations of *Apatosaurus* sp. (MOR 700), and *Diplodocus* sp. (CMC VP14128, MOR 592, and MOR 7029) reveal that all of these specimens possess a postparietal foramen (Figure 4). In some specimens, such as in *Apatosaurus* sp. (BYU 17096 and MOR 700) and *Galeamopus* (SMA 0011), the postparietal foramen appears to be immediately posterior to, or posteriorly connected to the frontoparietal fenestra, while in others the fenestra and foramen are spaced apart. The exact morphology of the foramen can be difficult to discern due to damaged margins, but in general it is ovoid in outline. In some specimens the foramen's greatest axis is transverse to the long axis of the skull (MOR 700), while in others it appears to be parallel to the long axis of the skull (SMA 0011; note this skull is damaged, so this morphology may be taphonomically altered).

Macroscopic examination of pneumatic structures in a proposed ontogenetic series. The smallest specimen examined in this study is SMA 0009, a specimen that was initially referred to Diplodocidae (Schwarz et al., 2007b) but that was later recovered as an immature brachiosaurid in phylogenetic analyses (Carballido et al., 2012; Tschopp et al., 2015). We follow Schwarz et al. (2007b) in considering this specimen a diplodocid and note that the forked [a.k.a. "sled"-shaped]

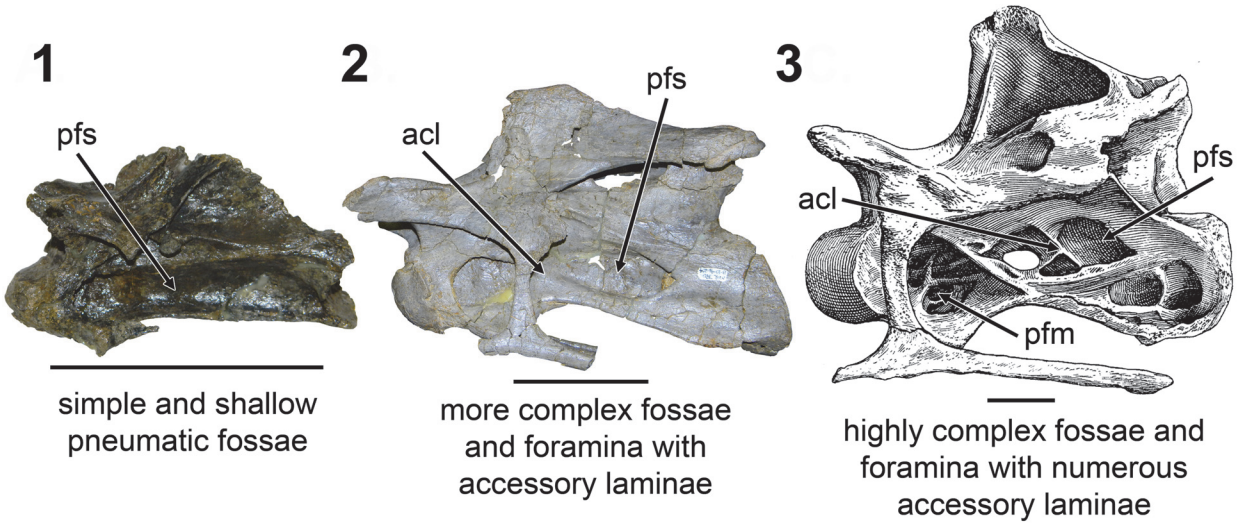

FIGURE 5. Macroscopic pneumatic architecture in diplodocid cervical vertebrae. **1,** diplodocid indeterminate MOR 714 7-22-3-53; **2,** *Diplodocus* sp. MOR 790 8-10-96-204; **3,** *D. carnegii* CM 84 (from Hatcher, 1901). Increasing pneumatic complexity from 1 to 3. pfs = Pneumatic Fossa, acl = Accessory Lamina, pfm = Pneumatic Foramen (Wedel, 2003). Not to scale. Scale bar equals 10 cm.

chevrons of SMA 0009 (which while coded by Tschopp et al. [2015], such morphology is not observed in *Camarasaurus* or *Brachiosaurus*) are further indicators of diplodocid affinity (although it is possible that chevron morphology changes ontogenetically [Otero et al., 2012], and "sled"-shaped chevrons are documented in basal sauropodomorphs). SMA 0009 represents an animal with an approximately 50 cm long cervical series. Our description of SMA 0009 follows that of Schwarz et al. (2007b). Macroscopically the cervical vertebrae appear acamerate (fossae do not invade centrum). The pneumatic fossae (not leading to internal chambers) of the cervical series are structurally simple, consisting of a shallow oval that extend for much of the length of each centrum. On the mid-cervical vertebrae the pneumatic fossae have an average depth of 4 mm, while in the posterior cervical the depth increases up to 8 mm. On the anterior and posterior cervical vertebrae, an accessory lamina divides the pneumatic fossae. On the anteriormost cervical vertebrae, this accessory lamina separates an anterior and posterior fossa; on the posteriormost cervical vertebrae these laminae are weakly expressed (Figure 5).

The next size range consists of individuals with a cervical series up to approximately 3 m in length. Individuals representing this size range, such as *Kaatedocus* SMA 0004, the *Apatosaurus* CM 3390, all exhibit procamerate to camerate (various degrees of pervading complexity into the centrum) cervical vertebrae. In this size class all of the pneumatic fossae are deepened and well defined. As in the previous size range, the fossae and foramina of the anterior cervicals are shallower than those in the posterior cervical vertebrae. The anterior fossae/foramina range from a depth of ~7 mm to 13 mm, while the posterior ones range from ~ 15 mm to as deep as 24 mm in SMA 0004. Additionally, the primary accessory laminae along with both the posterior centrodiapophyseal lamina and the postzygodiapophyseal laminae are more pronounced (Figure 5).

The next size range collectively represents the largest (and presumably sexually mature) specimens in the dataset. However, within this large size range, there are two discernible groups. The first group represents specimens with cervical series 4-6 m in length, such as the *Apatosaurus excelsus* (or *Brontosaurus excelsus*) CM 555 and the *Diplodocus* sp. specimen MOR 592. As in the smaller specimens, the fossae and foramina continue to increase in size and depth. Likewise, all of the associated laminae continue to grow. The final size range represents the mature condition. The primary difference observed within this collective range is the degree and abundance of fossae and foramina. In examining the *Diplodocus carnegii* CM 84, the degree and number of foramina and laminae is dramatically increased (Figure 5). The greatest concentrations of these laminae are still in the mid- and posterior cervical, but in this final condition, these features even proceed into the anterior portion of the cervical series. In some of these

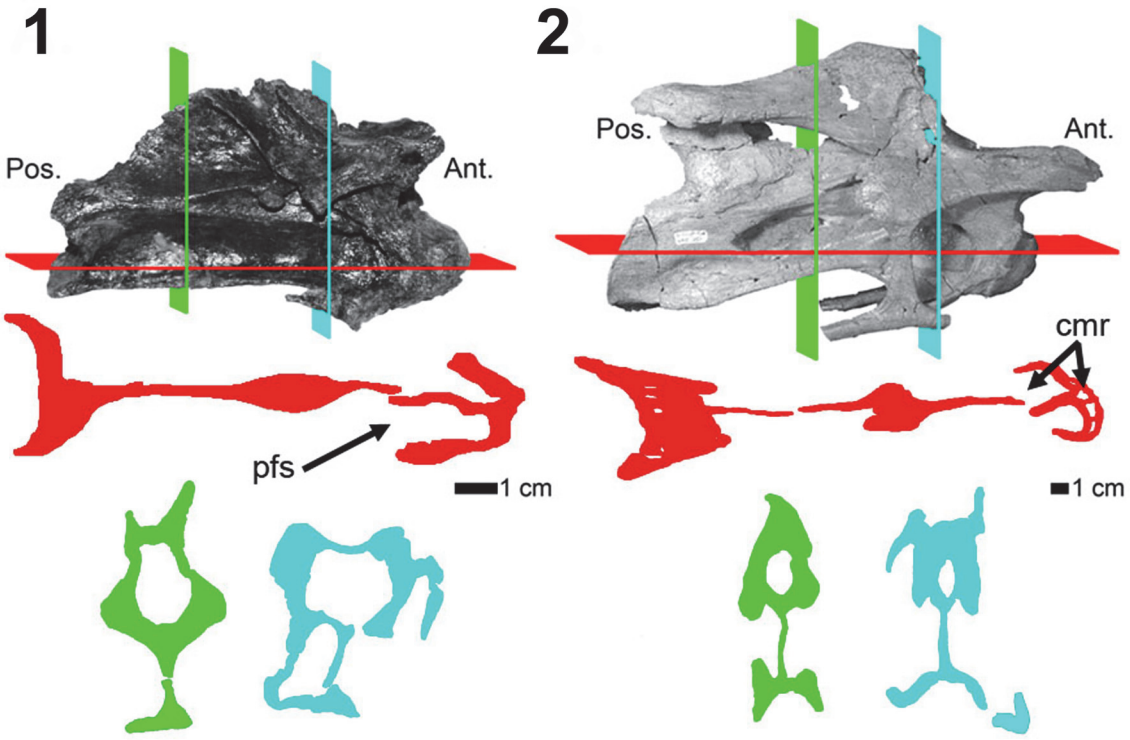

FIGURE 6. CT scans of diplodocid anterior cervical vertebrae. **1,** diplodocid indeterminate MOR 714 7-22-3-53; **2,** *Diplodocus* sp. MOR 790 8-10-96-204. Colored planes in 1 and 2 correspond to CT scan sections for each respective vertebrae. pfs = Pneumatic Fossa, cmr = Camera (Wedel, 2003). Red = frontal plane through the centrum, Blue = transverse plane through the anterior portion of the pfs, Green = transverse plane through the posterior portion of the pfs. Ant = anterior; Pos = posterior.

foramina-rich centra, such as C-11 of CM 84, the degree of laminae gives the appearance of a network of honeycomb.

Computed tomography. In the smallest anterior to middle cervical vertebra (diplodocid indeterminate MOR 714 7-22-3-53), the centrum is acamerate and appears to lack any secondary pneumatic structures. In both frontal and transverse views, the portion of the median septum bounded by the fossae has a fairly uniform thickness. Also in frontal view the lateral margins of the condyle are rather bulbous at their extremities. In the anterior to middle cervical vertebra of *Diplodocus* sp. MOR 790 8-10-96-204, we see in comparison to diplodocid indeterminate MOR 714 7-22-3-53 that the median septum has continued thinning. The most dramatic change is the pneumatic structures of the condyle; in frontal view the condyle has deep excavations, as in diplodocid indeterminate MOR 714 7-22-3-53, but in *Diplodocus* sp. MOR 790 8-10-96-204, the lateral margins of the condyle have continued to thin and taper. The bulk of the condyle is composed of large camerae (larger rounded cavities with a regular pattern) as observed in other sauropod condyles (Wedel, 2003; Schwarz and Fritsch, 2006; Schwarz et al., 2007a). The posterior portion of the cotyle also seems to possess camerae (Figure 6).

Collectively, the diplodocid dorsal vertebral series represent a more complete trajectory (in total consisting of five scanned vertebrae). In the anterior dorsal, *Diplodocus* sp. MOR 790 8-21-95-238, the median septum is uniformly thin and the pneumatic fossae extend deeply into the condyle. Both the condyle and cotyle of *Diplodocus* sp. MOR 790 8-21-95-238 are deeply penetrated by pneumatic fossae. It would also appear that internal pneumatic structures are nearly absent. In frontal view only one possible small camera is observed in the condyle. In the *Diplodocus* sp. MOR 592 8-22-90-75, there is continuing invasion of the pneumatic fossae into the condyle. Due to lateral shearing, the median septum is highly fragmented. In frontal view it would appear that *Diplodocus* sp. MOR 592 8-22-90-75 lacks any internal pneumatic structures. However, in transverse view there are several camerae and camellae (smaller angular cavities with an irregular pattern), primarily

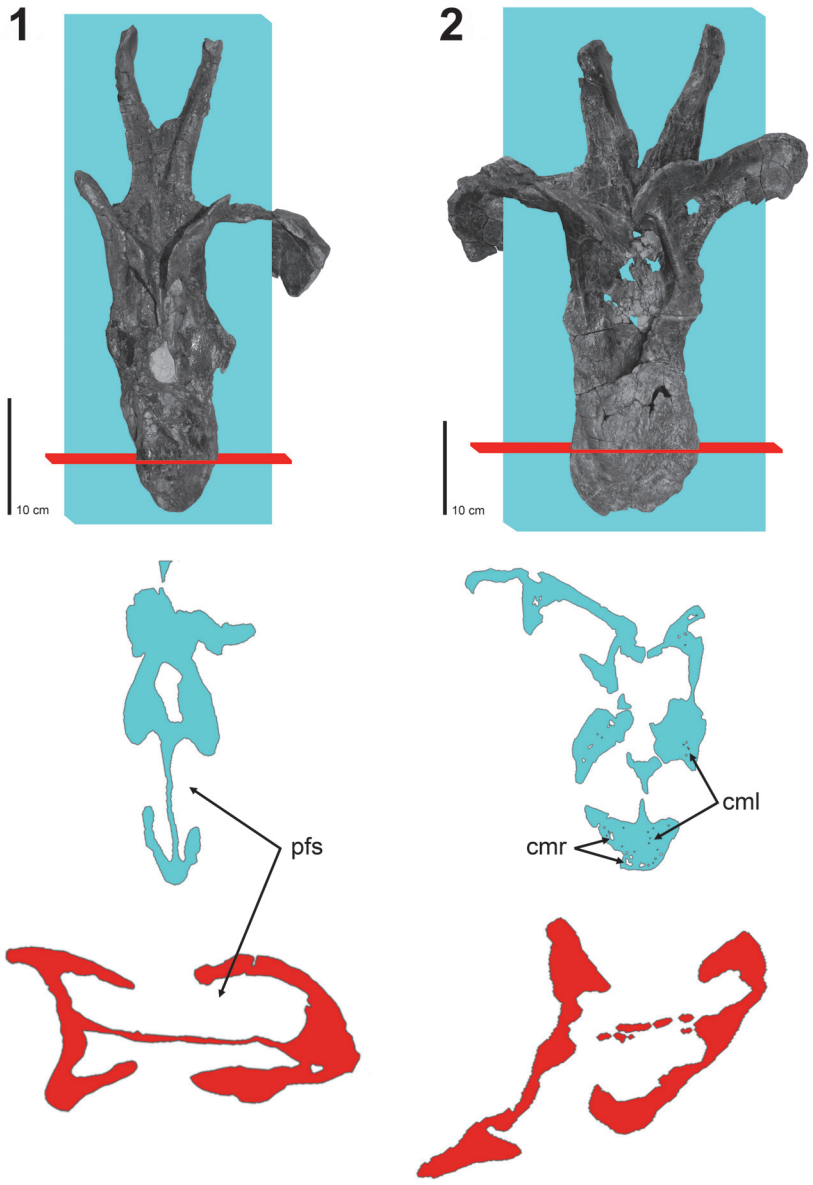

FIGURE 7. CT scans of diplodocid anterior dorsal vertebrae. **1,** *Diplodocus* sp. MOR 790 8-21-95-238; **2,** *Diplodocus* sp. MOR 592 8-22-90-15. Colored planes in 1 and 2 correspond to CT scan sections for each respective vertebrae. pfs = Pneumatic Fossa, cmr = Camera, cml = Camella (Wedel, 2003). Red = frontal plane through the centrum, Blue = transverse plane through the pfs.

along the peripheral margins of the centrum. *Diplodocus* sp. MOR 592 8-22-90-75 also marks the first appearance of pneumatic structures within the neural arch. Those in the arch would likewise appear to consist of camerae and camellae (Figure 7).

The posterior dorsal series exhibits perhaps the best ontogenetic development of the pneumatic structures. In examining the series developmentally, the *Diplodocus* sp. MOR 790 7-8-95-17 is structurally simple. The centrum is acamerate and lacks any sort of internal pneumatic structures (as hypothesized by Wedel, 2003). In addition, the medially shallow lateral fossae are separated by a very thick median septum. In the *Diplodocus* sp. MOR 592 8-22-90-77, the lateral pneumatic fossae extend medially into the centrum, producing a relatively thinner median septum. In addition to the thinning of the median septum, numerous internal pneumatic structures are present. The cotyle appears to consist of a complex of fairly interconnected camerae with some less numerous camel-

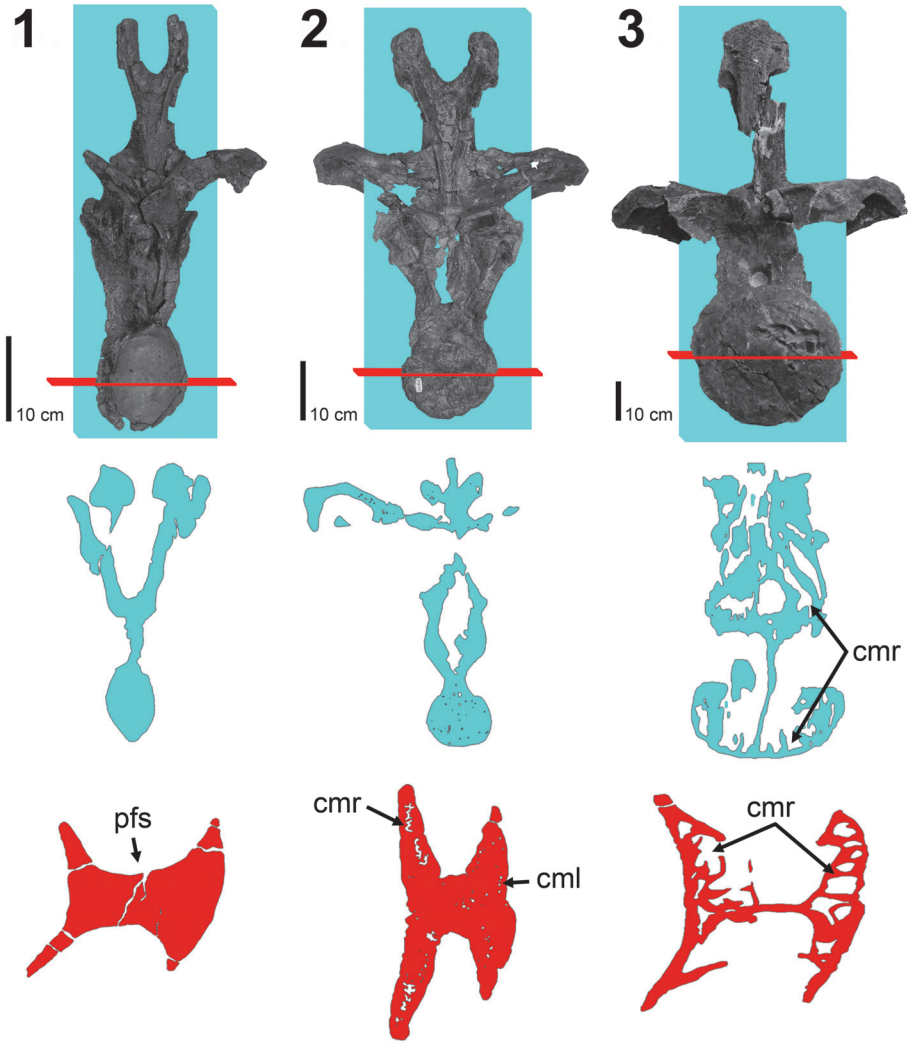

FIGURE 8. CT scans of diplodocid posterior dorsal vertebrae. **1,** *Diplodocus* sp. MOR 790 7-8-95-17; **2,** *Diplodocus* sp. MOR 592 8-22-90-77; **3,** *Apatosaurus* sp. MOR 957 6-29-92#1. Colored planes in 1, 2, and 3 correspond to CT scan sections for each respective vertebrae. pfs = Pneumatic Fossa, cmr = Camera, cml = Camella (Wedel, 2003). Red = frontal plane through the centrum, Blue = transverse plane through the pfs.

lae, whereas the condyle appears to contain primarily interspersed camellae. There also appear to be some small camerae and camellae in the neural arch. Progressing to the largest posterior dorsal vertebra in this series, *Apatosaurus* sp. MOR 957 6-29-92 29#1 is significantly larger than *Diplodocus* sp. MOR 592 8-22-90-77; unfortunately a suitable intermediate specimen was not available for study. The most notable feature of *Apatosaurus* sp. MOR 957 6-29-92 29#1 is the elaborate and extensive pneumatization. The lateral pneumatic fossae have extended deep into the centrum to produce a median septum that in certain locations is under 2 cm in thickness. In frontal view both the condyle and cotyle are completely composed of large (several cm in greatest length) extensive camerae. In transverse view there is even more apparent pneumatization. The thin median septum and large camerae of the centrum are evident, and the neural arch hosts a series of elongate camerae. These neural arch camerae gently arc medially towards the neural canal, and their overall size decreases dorsally while the dividing septa increase in thickness dorsally (Figure 8).

Ontogenetic Data

As histology is the only conclusive way to determine bone growth, multiple skeletal elements were sampled histologically.

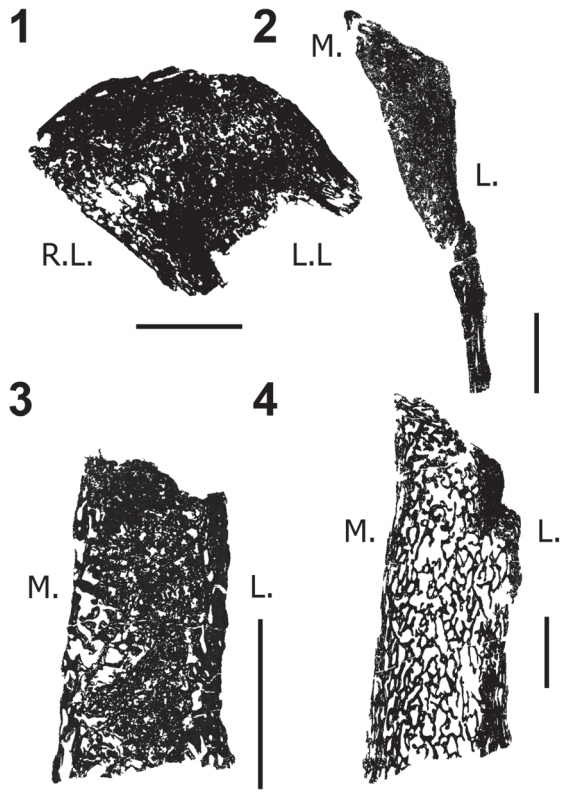

FIGURE 9. Coronal histologic sections of diplodocid posterior cervical and anterior dorsal vertebrae neural spines. **1,** Posterior cervical *Diplodocus* sp. MOR 790 (un-numbered 1); **2,** Anterior dorsal *Diplodocus* sp. MOR 790 8-21-95-238; **3,** Posterior cervical *Diplodocus* sp. MOR 592 8-24-90-91; **4,** Anterior dorsal *Diplodocus* sp. MOR 592 8-22-90-15. R.L. (right lateral), L.L (left lateral), M. (medial), L (lateral). Not to scale. Scale bar equals 1 cm.

Neural spine histology. In the posterior cervical of *Diplodocus* sp. MOR-790 (an un-numbered vertebra here designated un-numbered 1; and anterior dorsal of *Diplodocus* sp. MOR 790 8-21-95-238) the inter-trabecular spaces are small and generally divided into two size ranges: those well under 1 mm and those equal to or larger than 1 mm (however, in *Diplodocus* sp. MOR-790 un-numbered; here designated un-numbered 2; a few of the inter-trabecular spaces are up to 3.5 mm in greatest length; Figure 9). In the non-bifurcated *Diplodocus* sp. MOR-790 un-numbered 2, the apex of the undivided neural spine is more compact, with the bulk of the more cancellous bone loosely oriented in a convex arc across the width of the neural spine.

In the *Diplodocus* sp. MOR 790 8-21-95-238, the lateral margin is primarily compact bone with the more cancellous bone restricted to the medial margin of the split spine. This feature is likewise observed in the posterior cervical (8-24-90-91) and anterior dorsal (8-22-90-15) of *Diplodocus* sp. MOR 592. In the bifurcated *Diplodocus* MOR 592 8-24-90-91 there are two ranges of inter-trabecular sizes (far more of the larger spaces), and the spaces are distributed throughout the spine's apex (Figure 9). In addition, the lateral margin of *Diplodocus* sp. MOR 592 8-24-90-91 is more compact with the largest inter-trabecular spaces being restricted along the medial border. In *Diplodocus* sp. MOR 592 8-22-90-15 the inter-trabecular spaces are elongate and generally much larger than those from the previously discussed specimens (approximately 3 mm or larger). The lateral margin of the spine's apex is primarily compact with a more cancellous medial periphery. A much more complete ontogenetic series is needed to substantiate and correlate these results, but potentially these specimens suggest that throughout ontogeny, inter-trabecular spaces increase in size and orientation, and as bifurcation of the spine develops, so changes the degree and location of these bone types within the spine's apex.

Dorsal rib histology. The smallest (and presumably most immature) specimens sampled represent the size extremes recorded from the Mother's Day Quarry. The Mother's Day Quarry represents a bone bed of at least 15 immature diplodocids with femoral lengths between 102 and 120 cm. Unfortunately, the Mother's Day material is largely disarticulated and disassociated, so serial position or association is an approximation. If the femora extremes represent the minimum and maximum size range, we hypothesize that the smallest and largest anteriormost dorsal ribs likewise reflect these size extremes.

Within the smallest Mother's Day dorsal rib (*Diplodocus* sp. MOR 790 7-24-96-95; Figure 10), the bone microstructure is predominantly woven (highly disorganized, indicating fast growth). The bone is highly vascularized, and throughout there are numerous resorption cavities (~1 mm in greatest diameter). The vascular canal orientation throughout is principally longitudinal and reticular. In the vicinity of the anterior intercostal ridge, the periosteal cortex vascular canal orientation is uniformly longitudinal, while the medialmost portion transitions from longitudinal to reticular. Secondary osteons are principally located adjacent to the deep cortex trabecular bone and within the anterior intercostal ridge. This varying microstructural anatomy within a single section is why Waskow and Sander (2014) emphasize that dorsal ribs should not be cored; sampling in three different locations

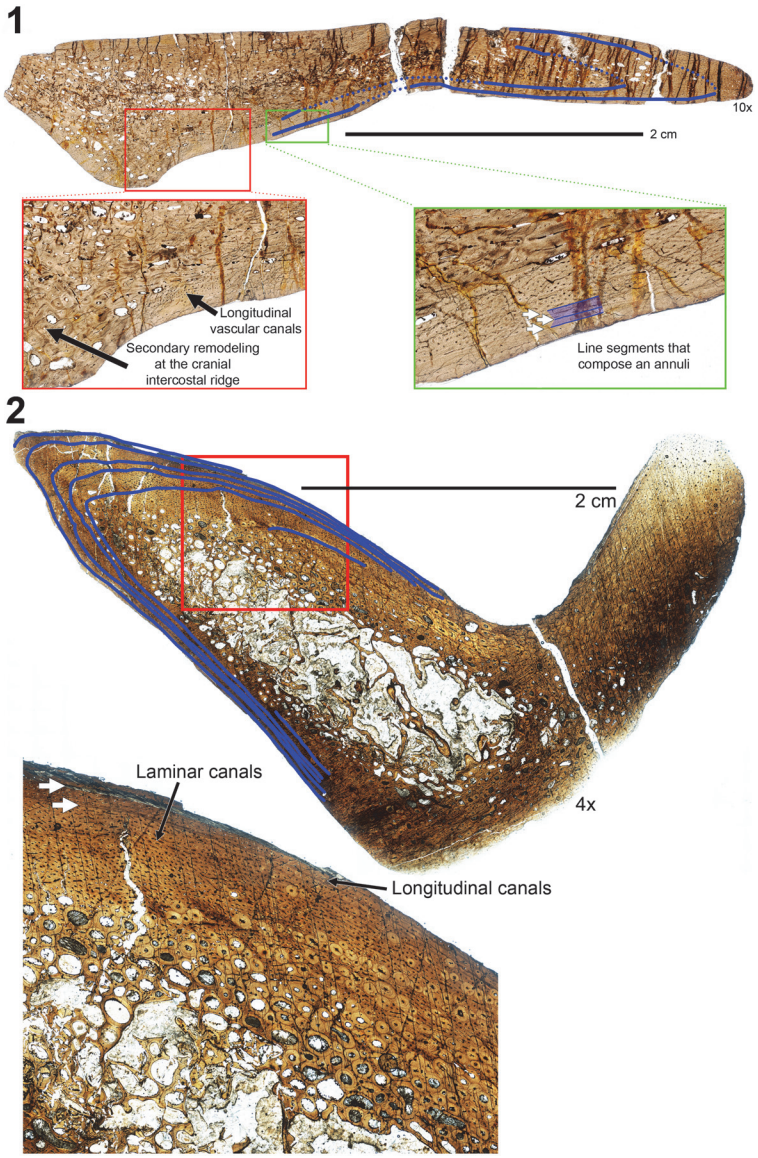

FIGURE 10. Transverse histologic sections of the H-MOS Stage 2 *Diplodocus* sp. **1,** MOR 790 7-24-96-95 (10x) and **2,** MOR 790 7-27-8-96 dorsal ribs (4x). **1,** MOR 790 7-24-96-95 records a minimum of two annuli (blue lines). Red insert box highlights bone microstructure differences between the anterior intercostal ridge and lateral margins with longitudinal vascular canals. Green insert box highlights a sample of the segments that comprise one of the growth markers (an annulus, highlighted in blue). **2,** MOR 790 7-27-8-96 records a minimum of six LAGs (blue lines; note some of these LAGs do extend past the demarcated blue lines). Red insert box highlights the microstructure and shows the vascularity patterns while the white arrows denote two of the LAGs present.

could yield three entirely different life history interpretations. While there are no continuous LAGs or indications of growth cessation, there are numerous smaller, semi-opaque, and non-continuous line segments. These segments are primarily concentrated into two distinct regions, and these regions collectively are much thicker than a LAG. Between these segments are smaller regions of slower, but continuous growth; as such we identify these regions as annuli (*sensu* Francillon–Vieillot et al., 1990). It must be explicitly stated that an annuli represent a slowing of osteogenesis, not an annual cessation (as in the case of LAGs; Castanet et al., 1992). Therefore, we infer that this individual records a minimum of two annual growth markers.

Since no annuli are observed further within the cortex, we would suggest that all – if not the majority – of the growth record is present. Alternatively it could be suggested that portions of the growth record may not be present (due to many

possibilities ranging from remodeling to cortical drift). The retrocalculation method of Waskow and Sander (2014) may be applicable in determining maximum age estimates. Waskow and Sander's (2014) retrocalculation methodology requires measuring the smallest and largest LAGs intervals and then marking off the distance until reaching the rib origin. While this methodology will prove incredibly useful in age estimation, such a methodology implies uniform growth (and the dinosaurian record explicitly argues against such). Using a modified version of Waskow and Sander's (2014) retrocalculation method, we used the greatest LAG spacing to calculate a maximum age estimate (this technique has been used for other sauropods [Woodruff and Foster, 2017]). Using this methodology we calculate an absolute maximum age of death of 7 years for MOR 790 7-24-96-95 (but we hypothesize this animal's actual age to be much closer to the histologic value).

The largest represented dorsal rib from the Mother's Day Quarry is *Diplodocus* sp. MOR 790 7-27-8-96 (Figure 10). Like the smallest Mother's Day specimen, *Diplodocus* sp. MOR 790 7-27-8-96 is highly vascularized with numerous resorption cavities (up to ~2 mm in greatest diameter). Adjacent to the deep-cortex trabecular bone is a relatively large (up to several mm in thickness) region of secondary remodeling. Within this lateral remodeled region, up to two generations of secondary osteons are observed. The remainder of the medial cortex is comprised of woven bone with a few secondary osteons infrequently dispersed. Endosteally the vascular canal orientation exhibits longitudinal and laminar regions, while the outermost cortex transitions from laminar to longitudinal canals. Like the smaller MDQ dorsal rib, the anterior intercostal ridge is highly remodeled and consists of Haversian bone comprising up to four generations of secondary osteons. *Diplodocus* sp. MOR 790 7-27-8-96 does preserve distinct and discernable LAGs. These preserved LAGs are largely restricted to the outer portion of the cortex (note not outermost, and therefore not an EFS), and there are a recorded minimum of six preserved LAGs (there may be up to three additional LAGs in the innermost cortex, but this region is highly remodeled, and these line sections are not continuous nor seen elsewhere, therefore we tentatively do not identify them as such). Using the age estimation methodology outlined above, we estimate a maximum age of death of 10 years for MOR 790 7-27-8-96.

The next size range is represented by the *Diplodocus* sp. MOR 592 (Figure 11). As in the MDQ dorsal ribs, the dorsal rib of the *Diplodocus* MOR 592 is highly vascularized with numerous resorption cavities. The anterior intercostal ridge is composed entirely of dense Haversian bone, however, the medial portion of the rib records pertinent life history information. Adjacent to the deep cortex trabecular bone, there is a large (approximately 2 cm) region of highly vascular, longitudinal, woven bone. This region is composed of longitudinal vascular canals arranged in radial rows (*sensu* Francillon-Vieillot et al., 1990). Immediately adjacent to this highly vascularized longitudinal region for the remainder of the cortex is an area of less vascularized primary bone. In this outermost region the vascular canal orientation changes from longitudinal to reticular. The dorsal rib of *Diplodocus* sp. MOR 592 records a minimum of eight observable LAGS; however, no LAGs are visible within or prior to the highly vascularized longitudinal area. In using the aforementioned age estimation technique, we estimate a maximum age of death of 12 years for MOR 592.

The final and largest specimen is represented by the paratype of *Diplodocus carnegii* (CM 94; Figure 12). As in all of the aforementioned dorsal ribs, that of CM 94 is highly vascularized and possesses a dense network of deep-cortex trabecular bone. However, unlike the previous dorsal ribs, that of CM 94 has proportionally a much larger and more extensive area of secondary remodeling (laterally up to three generations of secondary osteons) adjacent to the deep cortex trabecular bone. The periosteal portion of the cortex is comprised of fibrolamellar bone. The vascular canal orientation of the entire section is longitudinal. No radial regions are observed in CM 94. Regions of longitudinal vascular canals are bracketed by LAGs; these canals are found in episodic groupings of either predominantly larger (mean canal diameter 86.50 μm) or smaller (mean canal diameter 47.30 μm) vascular canal diameters. Perhaps these bands are representative of episodic growth. Within the outermost four to five mm of the cortex there is a decrease in vascularity, which is represented by the occurrence and size of vascular canals. The dorsal rib of CM 94 records a minimum of 24 countable LAGs. In addition to the high LAG count, the outermost portion of the cortex records 3-4 closely spaced LAGs in low vascularized tissue. We believe that this region is an external fundamental system (EFS; the histologic indicator of growth cessation). The presence of an EFS in the dorsal ribs indicates that CM 94 was skeletally mature (and potentially the same may hold true for

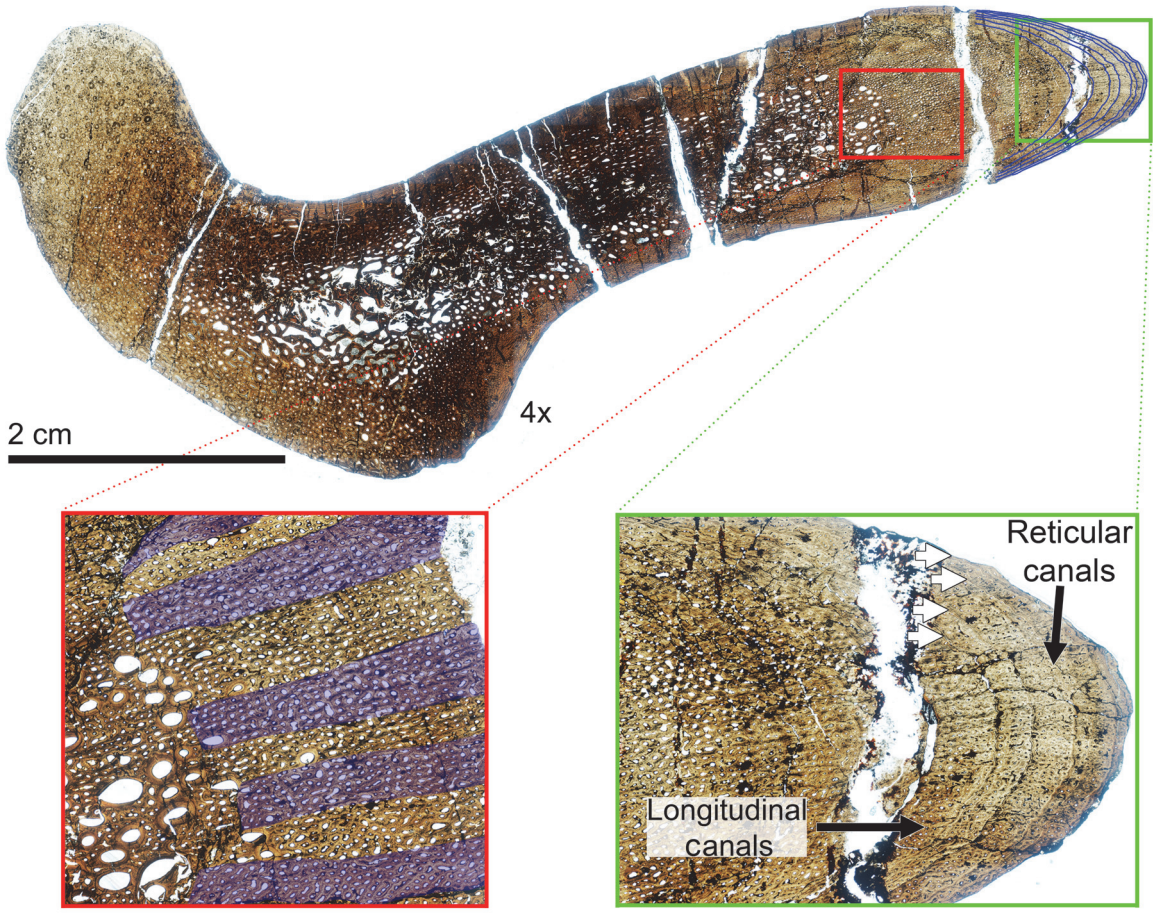

FIGURE 11. Transverse histologic section of the H-MOS Stage 3 *Diplodocus* sp. MOR 592 dorsal rib at 4x. MOR 592 records a minimum of eight LAGs (blue lines). Red insert box highlights the organization of longitudinal vascular canals in radial rows (alternating rows highlighted in blue). Green insert box highlights the vascularity patterns with white arrows denoting four of the LAGs present.

the slightly larger holotype CM 84), and therefore these size ranges do indeed represent the previously assumed skeletally mature sizes of *D. carnegii.* And in calculating the maximum age estimate, we estimate a maximum age of death of 34 years for CM 94.

Femoral Histology

Mother's Day Quarry femora. The work of Klein and Sander (2008) suggests a linear relationship between femoral length and HOS in sauropods. Thus, this trend indicates that the largest femur from the monospecific Mother's Day Quarry (*Diplodocus* sp. MOR 790 7-23-95-122, 120 cm long; Figure 13) represents the oldest animal from the quarry. With a complete cortex 11.29 mm thick, endosteally the medullary region contains large resorption cavities, while periosteally the mineralized tissue grades from Haversian bone into a scattered region of remodeling. Further periosteally, the remainder of the cortex comprises a very thin unit of Types D and E bone (*sensu* Klein and Sander 2008). Klein and Sander (2008) report that growth marks may appear in Type E bone (although extremely rare); however, no growth marks are visible in MOR 790 7-23-95-122. The histology indicates that MOR 790 7-23-95-122 presumably the most skeletally mature individual from this locality represents HOS 7 out of 13.

MOR 592 femur. The medullary cavity of the *Diplodocus* sp. MOR 592 (femur length 124.5 cm) is large with the complete cortex 29.51 mm thick (Figure 14). From the medullary cavity there is a large zone of Haversian bone, while periosteally, remodeling becomes less frequent within the primary tissue. Type E bone predominates for the remainder of the cortex. In the case of the MOR 592 femur, at least one LAG is present along the

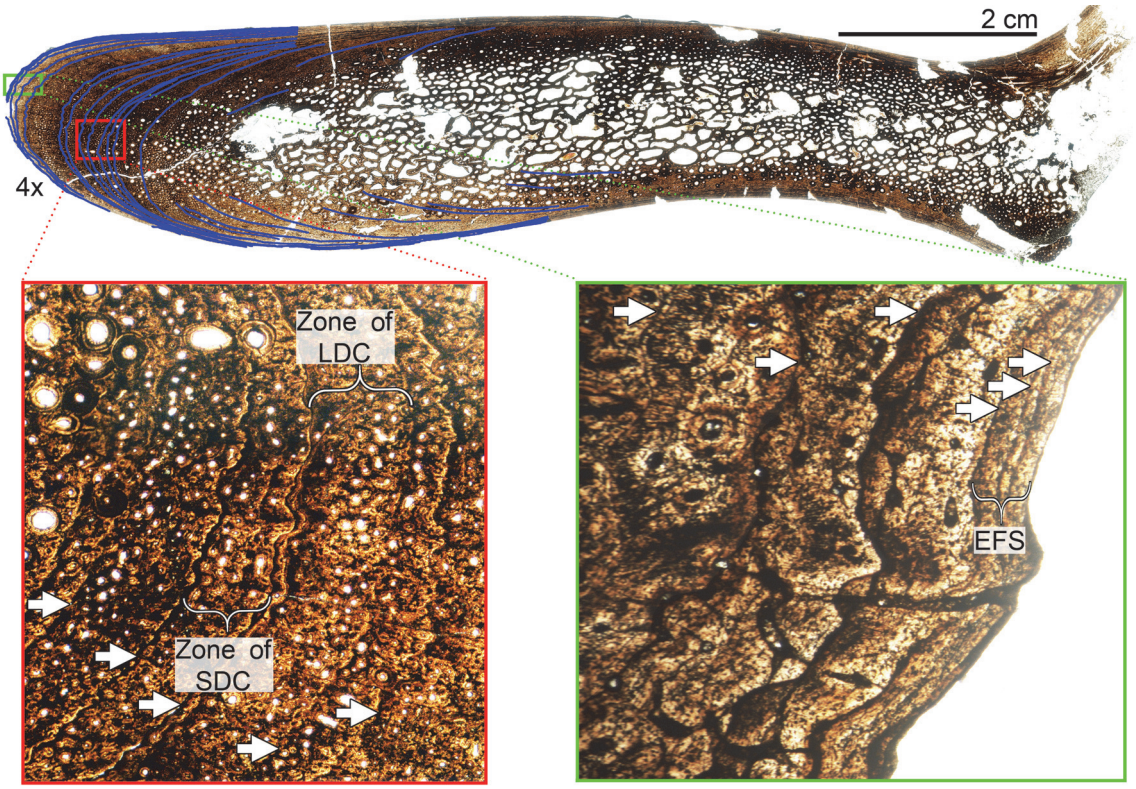

FIGURE 12. Transverse histologic section of the H-MOS Stage 4 *Diplodocus* CM 94 (*Diplodocus carnegii* paratype) dorsal rib at 4x. CM 94 records a minimum of 24 LAGs (blue lines). Red insert box highlights the episodic zones of large (LDC) and small (SDC) diameter longitudinal vascular canals with white arrows denoting some of the LAGs present. Green insert box highlights the outermost cortex which records the presence of an EFS. White arrows denote LAGS present, with the EFS bracketed.

periosteal margin. MOR 592 representing HOS 9 out of 13 is consistent with femoral length versus HOS correlations found by Klein and Sander (2008). The lack of a cortex consisting entirely of Haversian bone and the lack of an EFS indicates that skeletally, MOR 592 is immature (Figure 14). Klein and Sander (2008) and Gallina (2011, 2012) correlate HOS 9 with sexual maturity in sauropods. While vertebrate reproductive biology favors the onset of sexual maturity prior to skeletal maturity (van Tienhoven, 1983), no histologic indicators of sexual viability was observed (e.g., medullary tissue), therefore, we will not address the reproductive nature of MOR 592. Thus osteohistology supports the conclusions of Woodruff and Fowler (2012) that MOR 592 is skeletally immature.

DISCUSSION

Morphologic Evidence

Pneumatic architecture. Wedel (2005) demonstrated the importance and implications of pneumaticity in sauropod vertebrae (particularly in regards to mass estimations). In regards to quantifying the pneumatic potential, Wedel (2005) proposed the calculation of the air space proportion (ASP) - the volume of air versus the volume of bone. The ASP methodology is simplistic and relies on a two-color image. One color delineates the volume of the bone in cross-section, and the other color represents the area filled by pneumatic structures (see Wedel [2005] for details). A simple calculation comparing the pixel count of bone to air will result in an ASP value. Out of the spectrum of sauropods examined, Wedel (2005) and Wedel and Taylor (2013) had a degree of variability, but noted that most sauropod vertebrae contained approximately 60% empty space by volume, comparable to avian ASP values. Additionally Wedel (2005) noted that the execution of ASP was still in its infancy; the location of the section in a given vertebra and the serial position could greatly affect the calculated ASP. However, Wedel (2003, 2005, 2009) demonstrated that vertebral pneumatic complexity has increased through sauropodomorph

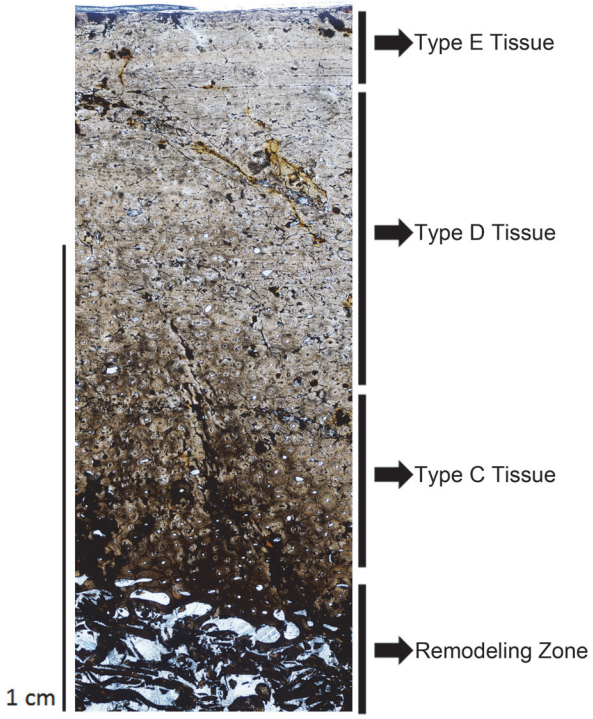

FIGURE 13. Transverse histologic section of the H-MOS Stage 2 *Diplodocus* sp. MOR 790 7-23-95-122 femur at 4x. MOR 790 7-23-95-122 is HOS 7 out of 13. No LAGs are present.

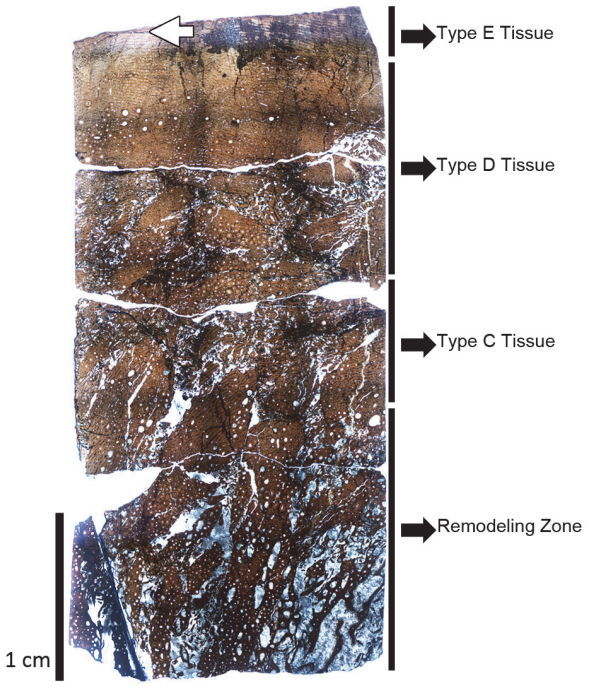

FIGURE 14. Transverse histologic section of the H-MOS Stage 3 *Diplodocus* sp. MOR 592-35 femur at 4x. White arrow marks one observable LAG. MOR 592 is HOS 9 out of 13.

phylogeny. Thus ASP increases in tandem with pneumatic complexity.

ASP is an important character, but, in this analysis, we felt cautious about the quantification of ASP. For the CT-scanned vertebrae, we attempted to view transverse slices near the mid-point of the pneumatic foramen and sagittally through the length of the centrum. In viewing the scan data, the anterior and posterior pneumatic foramen slices vary, so in calculating ASP, perhaps an average from multiple fixed locations would give an overall vertebral ASP. Regardless of the quantified ASP, in examining the scan data, one can clearly see (particularly within the dorsal vertebrae) that the pneumatic architecture increases in complexity throughout ontogeny (Wedel, 2003; Schwarz et al., 2007a; Carballido and Sander, 2014). An additional ASP consideration is that patterns in dorsal pneumaticity appear to be associated with avian-style respiration (Wedel, 2003; Schwarz et al., 2007a; Wedel, 2009; Melstrom et al., 2016). Thus differing dorsal ASP between two taxa could be related to variation in the degree of respiratory tissue, rather than to ontogeny or phylogeny. Quantifying the ASP will be important in regards to comparing taxa and calculating evolutionary trends; based on the preliminary data, we see that the complexity follows a developmental trajectory.

Interestingly, while the scans reveal general pneumatic architecture, we would stress they are not a true 1:1 reflection of the actual pneumatic morphology. When the *Diplodocus* sp. MOR 592 8-22-90-75 was scanned, the results showed that the neural spine had a dense outer cortex with a less dense interior. Within the neural spine there were only a few laterally restricted, small inter-trabecular spaces. Yet thin-sectioning revealed a completely different outcome. The dense periostealmost margin was verified, but the entirety of the internal aspect was instead occupied by cancellous bone with large inter-trabecular spaces. This discrepancy is best explained as an issue with scan resolution (the resolution in this study ranged from 2 mm to 5 mm) – smaller features could become less distinguishable with lower resolution, and density of infilled matrix could likewise cause visual obstruction. Rescanning at finer resolution, intensified contrast, differing can algorithms, or different scan filters could each clarify some of these issues. In addition to these possible adjustments, a comparative study examining the results between scan

images and complete histologic sections of each vertebra would be worthwhile.

Cranial foramen. Regarding the significance of the postparietal foramen, Harris (2006a) has suggested that this foramen was used for photoreception (i.e., a pineal eye). While relatively complete diplodocid skulls are rarely preserved, available specimens under ~40 cm in length all possess a postparietal foramen. Larger and presumably more mature diplodocid skulls (such as CM 11161 [*Diplodocus longus* or diplodocid indeterminate], USNM 2672 [*Diplodocus* sp. or diplodocid indeterminate], USNM 2673 [*Diplodocus* sp. or *Galeamopus*], and CM 11162 [*Apatosaurus louisae*]; however note that some of these skull are taphonomically altered) all lack this foramen. The presence/absence of this foramen between less and more mature individuals would suggest that, among Diplodocidae, the postparietal foramen is an ontogenetically variable cranial feature (Woodruff and Fowler, 2012; Woodruff et al., 2013; Woodruff and Fowler, 2014; Figure 4).

As the developmental pathway of the postparietal foramen has yet to be examined, it raises the question as to the proper terminology to be used in addressing this feature. Among the immature diplodocid skulls with this feature, it would appear that it initially represents a posterior opening between the sutural margins of the parietals (~1cm), and that through ontogeny this gap is reduced by the fusing parietals. By definition a foramen is a static opening (Grey, 1858), so with regard to the diplodocid condition, foramen is not an appropriate term. Hopson (1979) concluded that this cranial “foramen” was actually a fontanelle. A fontanelle is defined as the temporary membranous gap between developing cranial bones (Grey, 1858). If this feature is indeed ontogenetically variable among diplodocids, then fontanelle would be the more appropriate term. However, the cranial ontogeny of dicraeosaurids is currently unknown. It is possible that this group retains this cranial opening throughout ontogeny (paedomorphic) – thus it is a foramen, while in diplodocids this trajectory could be a peramorphic fontanelle, therefore neither term is suitable for referring to all sauropods. In lieu of a histological examination which could elucidate the proper terminology, we suggest using Balanoff et al.’s (2010) more neutral phrasing of “postparietal aperture”.

Femoral proportions. The large dataset for femora acquired for diplodocid body-mass estimations has likewise allowed for the examination of femoral ontogeny (Figure 15). Some studies suggest that sauropod limbs may have ontogenetically developed in a more isometric manner (Wilhite and Curtice, 1998; Wilhite, 1999, 2003; Bonnan, 2004; Rogers et al., 2016). Yet examining the dataset, allometric trends are observed. These allometric trends appear to apply to both *Diplodocus* and *Apatosaurus*. In many immature individuals the femoral head appears inclined at a greater angle to the long axis of the diaphysis (more pronounced in *Diplodocus*), and in the larger and more mature specimens the femoral head angle becomes more perpendicularly oriented. Similarly the medial condyle becomes much more pronounced (especially in *Apatosaurus*) in the larger and more mature individuals. Finally, with regard to femoral proportions, in the immature diplodocids the fourth trochanter is situated proportionally more proximally, while in more mature individuals, this trochanter is generally situated at approximately the mid-point of the diaphysis (Figure 15). A thin-plate spline analysis (such as those used in Wilhite and Curtice, 1998; Wilhite, 1999, 2003; Bonnan, 2004), or a geometric morphometric analysis via a principle component analysis (PCA), would be required to accurately quantify these changes and to possibly detect other proportional changes. Furthermore, since the fourth trochanter is an important attachment site for locomotory muscles (e.g., the *m. caudofemoralis longus*), the positional change of this anchoring point may affect the moment arm of such muscles, and subsequently, such changes may have gait or other biomechanical implications. While we await such analyses, we hypothesize that these differing femoral changes are indicative of allometric development.

Neural spine bifurcation. As most recently documented by Woodruff (2016) and echoed and noted by others, neural spine bifurcation is a complex vertebral adaptation (Thompson, 1942; Borsuk-Bialynicka, 1977; Bakker, 1986; Salgado and Bonaparte, 1991; Stevens and Parrish, 1999, 2005a; Dodson and Harris, 2001; Christian, 2002; Tsuihiji, 2004; Schwarz et al., 2007a; Senter, 2007; Schwarz-Wings and Frey, 2008; Seymour, 2009; Schwarz-Wings, 2009; Taylor et al., 2009; Wedel and Taylor, 2013). While there is a general consensus for a biomechanical origin, how (and if) it develops is a more contentious point. Amongst the diplodocids of the Morrison Formation that possess bifurcated spines (those represented by several specimens, thus excluding *Kaatedocus* and *Galeamopus*), the variabilities and degrees of bifurcation vary considerably – extremely long cervical series with a small degree of bifurcation (*Barosaurus*) to

FIGURE 15. Selection of the diplodocid femoral dataset used throughout this ontogenetic analysis. Top row diplodocines, from left to right: CM 33991 (*Diplodocus longus*), CM 21788 (*D. longus*), CM 30762 (*D. longus*), MOR 790 7-5-97-7 (*Diplodocus* sp.), MOR 790 7-23-95-122 (*Diplodocus* sp.), MOR 592-35 (*Diplodocus* sp.), CM 21752 (*Diplodocus* sp.), SMA 0013 (*Diplodocus* sp.), CM 84 (*D. carnegii*); Bottom row apatosaurines, from left to right: AMNH 613 (*Apatosaurus* sp.), OMNH 1279 (*Apatosaurus* sp.), AMNH 606 (*Apatosaurus* sp.), MWC 5439 (*Apatosaurus* sp.), CM 21784 (*A. louisae*), CM 33997 (*A. louisae*), MOR 700 7-24-91-31 (*Apatosaurus* sp.), AMNH 353 (*Apatosaurus* sp.), SMA 0014 (*Apatosaurus* sp.), CM 85 (*Apatosaurus* sp.), MOR 857 7-16-92-30 (*Apatosaurus* sp.), MWC "Moffit Co. Apato." (*Apatosaurus* sp.). Scale bar equals 1 m. Note the colored line on CM 84 and MWC "Moffit Co. Apato." illustrate how femoral positions and trends were examined. Colored lines to the far right of each row indicate the general allometric changes of each femur scaled to the same length (Black line = femoral length). *Diplodocus* row: Yellow lines = MOR 790 7-5-97-7, Blue lines = MOR 592-35, Red lines = CM 84. *Apatosaurus* row: Green lines = AMNH 613, Yellow lines = CM 33997, Blue lines = MOR 700 7-24-91-31, Red lines = MWC "Moffit Co. Apato."

shorter series with extreme bifurcation (*Apatosaurus*). The varying degrees of neural spine bifurcation dictate differing vertebral mechanics, and thus the development of this feature should likewise vary. If spine bifurcation is a product of vertebral biomechanics (Woodruff, 2014), then as the vertebral series increases in size (length and mass), then the mechanical stresses enacted upon the series adjust as well. Thus neural spine bifurcation is not considered ontogenetic in our most typical sense – it is not a feature that develops in tandem or coincides with pivotal life history events (i.e., sexual maturity). Instead, neural spine bifurcation can develop as the vertebral series increases in size (i.e., can change as the animal increases in size during growth). While the degrees and specifics pertaining to neural spine development appear to vary amongst these Morrison taxa, the agreeable theme is that the morphology of the bifurcation varies developmentally across ontogeny (i.e., can be absent to weakly expressed in smaller immature animals, while present or enhanced development in larger mature individuals, Figure 3).

Implications Regarding Sauropod Growth Rates

Results of the histologic examination of dorsal ribs indicate that these individuals grew rapidly. An

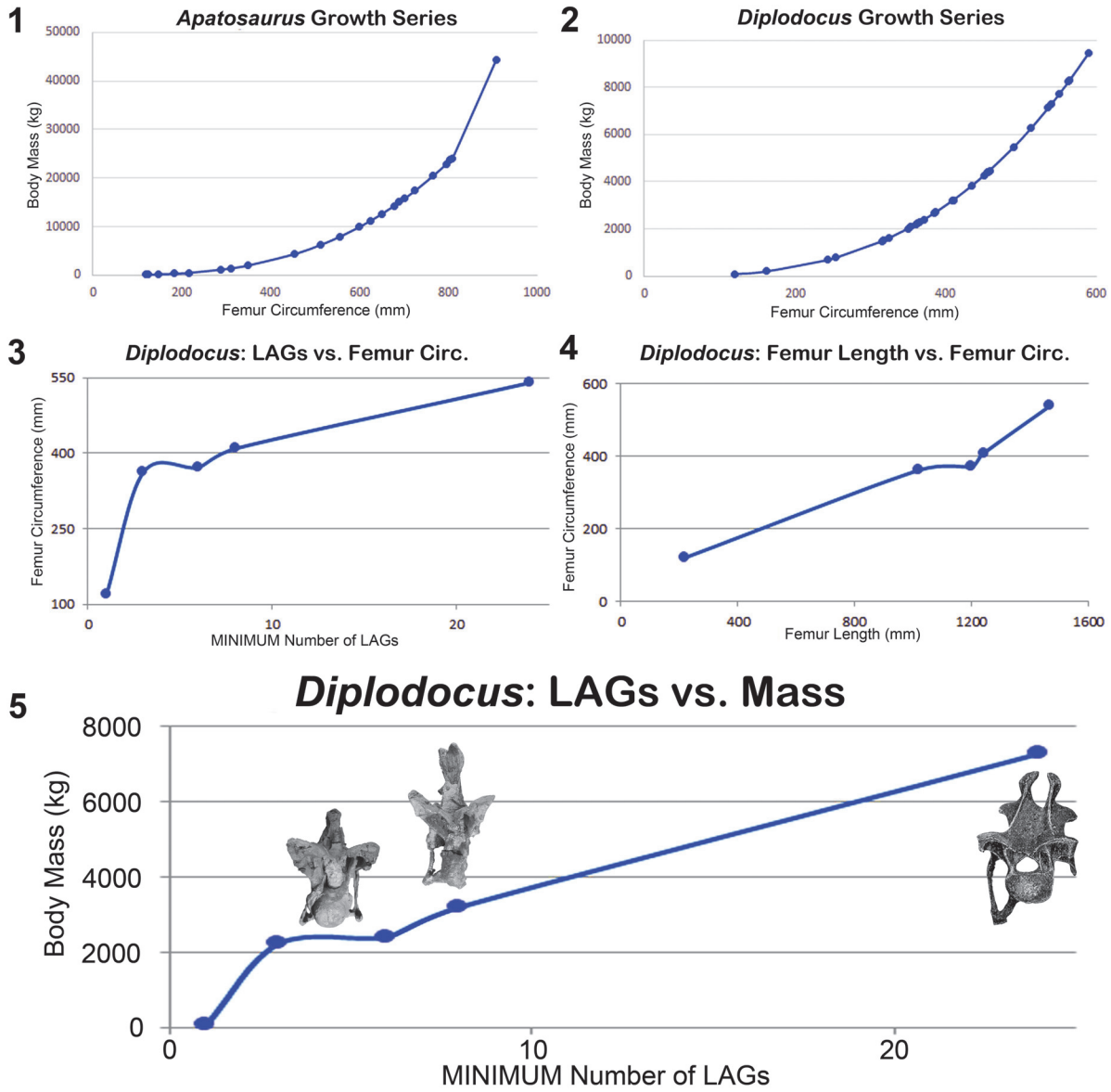

FIGURE 16. Calculated body masses for the Morrison diplodocids *Apatosaurus* (**1**) and *Diplodocus* (**2**) using the formula of Mazzetta et al. (2004) (log Body Mass = 2.955 x log Femur Circumference − 4.166); **3**, Dorsal rib LAG count vs. femur circumference for *Diplodocus*; **4,** Femur length vs. femur circumference for *Diplodocus*; **5,** Dorsal rib LAG count vs. body mass for *Diplodocus* with posterior cervical vertebrae marking each size range to illustrate the correlation between mass and spine morphology. Data for all diplodocid specimens can be found in Appendix 3.

immature diplodocid that is approximately 6 m long is at least six years old (such as *Diplodocus* sp. MOR 790 7-23-95-122), while a 27 m individual is at least 24 years old (*D. carnegii* CM 94). These growth rates are not nearly as accelerated as those recorded in some other dinosaurs - such as a 3 m body lengths within the first year in *Maiasaura* (Woodward et al., 2015) – but they are still consistent with rapid growth rates. In terms of historical perceptions of longevity, sauropods have run the estimation gamut – attaining maximum body size within a decade (Curry, 1999) or taking up to several centuries (and finally sexually mature at 72 years of age; Case, 1978). This variability in longevity estimates has allowed for practically every possible life history strategy to be proposed, and there is little consensus (at least modern studies agree the century estimates to be erroneous; Curry, 1999; Sander, 2000; Erickson et al., 2001; Sander and Tückmantel, 2003; Sander et al., 2004; Rogers and Erickson, 2005; Lehman and Woodward, 2008; Woodward and Lehman, 2009; Grie-

beler et al., 2013; Waskow and Sander, 2014). Studies that examine multiple aspects of ontogenetic data (e.g., Woodward and Lehman, 2009; Myhrvold, 2013; Hone et al., 2016) represent more comprehensive assessments of growth. For instance, by estimating both limb length and body mass for each LAG interval and applying this data into the von Bertalanffy growth equation, the life history of an individual *Apatosaurus* could be extrapolated (Woodward and Lehman, 2009).

Dorsal rib and femoral data allow for the formulation of hypotheses regarding mass-based ontogenetic trends in diplodocids. The femoral data applied to the Mazzetta et al. (2004) limb-bone allometry-based formula can calculate projected body masses. Morphologic features can be applied to the graph to determine the mass- and age-based timing of ontogenetic events (Figure 16). If the age-determining histology from the Mother's Day Quarry (*Diplodocus* sp. MOR 790) specimens is correct, then these animals are collectively under approximately 2,400 kg and around six years of age. The next range approximately represents the change to a taller and incipiently bifurcating spine apex, and this would seem to correlate with animals equal to or greater than 3,500 kg and a minimum of eight years of age. Finally, the mature stage comprises animals with fully bifurcated cervical spine apices and with weights of approximately 7,000 kg and at least 20 years of age. If these categorizations are correct, it would appear that the biomechanical stresses enacted upon the vertebral column change through ontogeny within *Diplodocus*, thus the degree of neural spine bifurcation was directly correlated with mass.

The recognition of such has extreme implications towards reconstructing the paleobiology of *Diplodocus* (and potentially other diplodocids). Immature *Diplodocus* (collectively under 2,400 kg and six years of age) had short, un-bifurcated neural spines, and quite differing cranial morphologies (such as a rounded "snout" and an elongated tooth row; Whitlock et al., 2010). These cranial changes have been suggested to indicate ontogenetic dietary partitioning (Whitlock et al., 2010), thus the evidence suggests that immature *Diplodocus* were at least feeding on different vegetation types. The combination of cranial and vertebral changes could be used to suggest that not only were immature *Diplodocus* feeding on differing plants types, but they might also have employed a differing feeding style (i.e., not lateral sweep feeding). As Woodruff (2016) demonstrated via anatomical comparisons to extant quadrupedal, terrestrial herbivores with bifurcated neural spines, the bifid spines serve as the attachment sites for a split nuchal ligament, with the interspinal ligament occupying the trough of bifurcation. The split nuchal ligament and other soft tissues associated with bifurcated spines, not only provide support against vertebral sagging and torsion, but provide elastic rebound (Woodruff, 2016). The split nuchal ligament provides lateral elastic rebound in the cervical series, which supports the lateral sweep feeding hypothesis of Stevens and Parrish (1999). However, a bifurcating spine affects far more than just the nuchal and interspinal ligament. For instance, increasing the spine height alters the size, area, and attachment of muscles which in turn alter the mass and lever arm of the vertebral series. Therefore all of the anatomical variables of the vertebral column have to change throughout ontogeny. The lack of bifurcated spines in very immature *Diplodocus* could support the theory that such animals were not laterally sweep feeding, although a mechanical analysis such as performed by Stevens and Parrish (1999) must be conducted to substantiate such.

Regarding growth rate, the morphologic data of this analysis suggests that *Apatosaurus* achieved a significantly greater body mass throughout ontogeny compared to *Diplodocus* (Figure 16). An age determining examination of *Apatosaurus* has yet to be conducted, but we hypothesize that *Apatosaurus* had a faster growth rate than *Diplodocus*. If one were to only examine *Apatosaurus* and *Diplodocus*, the degree of spine bifurcation would appear to be solely linked to body (or cervical) mass. While based on the relation between spine morphology and body mass, perhaps an immature *Apatosaurus* possessed greater spine bifurcation earlier in ontogeny than a similarly aged *Diplodocus*. We hypothesize that body mass is not the only factor influencing spine bifurcation (mobility of the cervical column being perhaps the most significant variable; Stevens and Parrish [1999, 2005a, 2005b]).

Questionable Small-Statured Diplodocid Taxa

Previous studies on diplodocid ontogeny have examined the validity of small-statured taxa such as *Suuwassea* (ANS 21122; Whitlock and Harris, 2010; Woodruff and Fowler, 2012; Wedel and Taylor, 2013; Hedrick et al., 2014; Tschopp et al., 2015). In the case of *Suuwassea*, the combination of basal and derived traits has explanatorily ranged from environmental adaptations (Harris, 2006b) to indications of immaturity (Woodruff and Fowler, 2012). Taxonomic placement of *Suuwassea* has

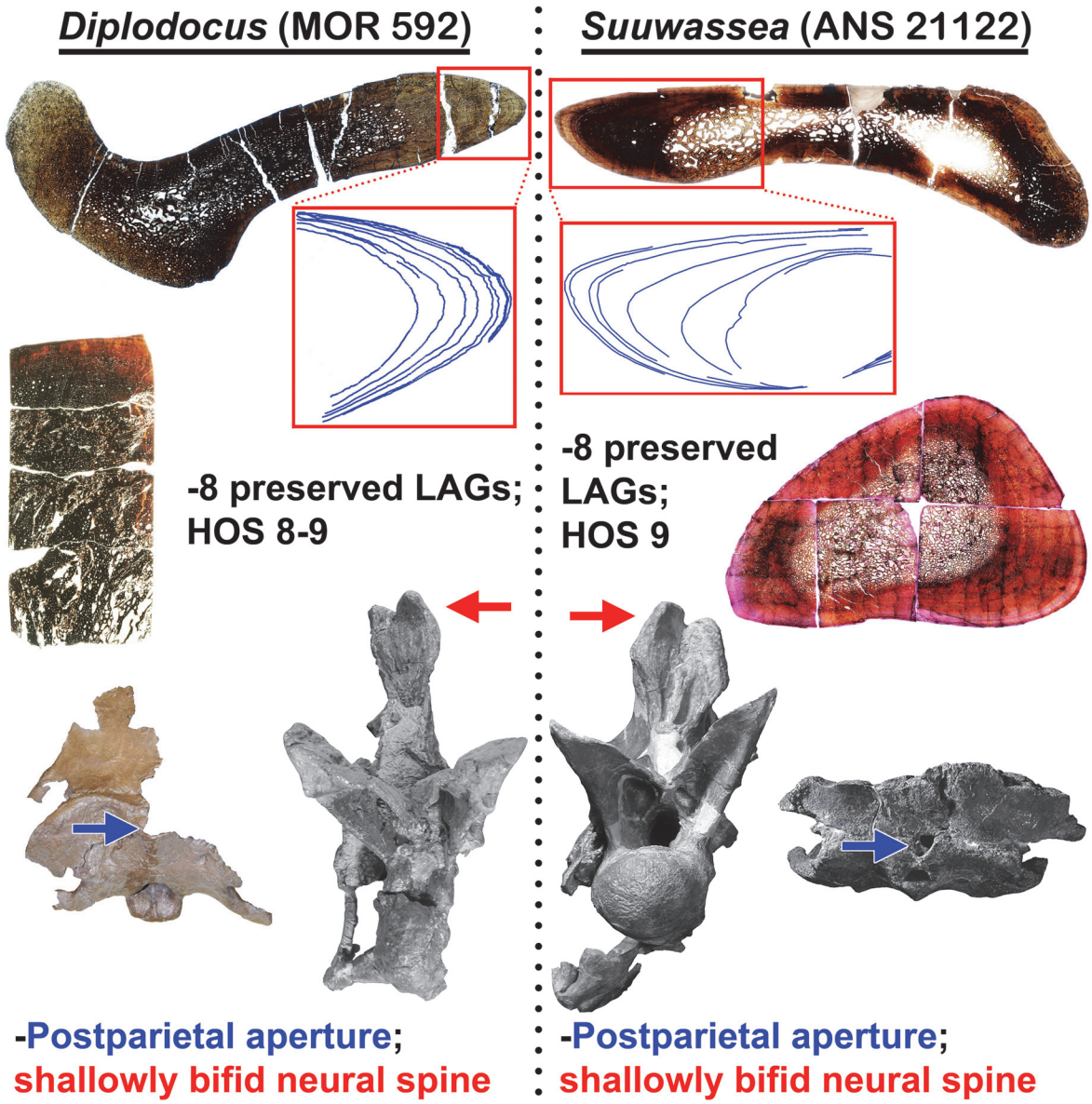

FIGURE 17. Histologic and morphologic commonalities of *Diplodocus* sp. (MOR 592) and *Suuwassea emilieae* (ANS 21122) which demonstrate immature maturational states for both animals (H-MOS Stage 3). Histologic section of *Suuwassea* tibia from Hedrick et al. (2014). The *Suuwassea* tibia histologic section is from *Acta Palaeontologica Polonica,* articles are distributed under the terms of the Creative Commons Attribution License (CC BY), which permits unrestricted use, distribution, and reproduction in any medium, provided the original author and source are credited. For licence details please see http://creativecommons.org/licenses/by/4.0/.

ranged from a basal apatosaurine (Harris and Dodson, 2004), a Laurasian dicraeosaurid (Whitlock and Harris, 2010; Wedel and Taylor, 2013; Tschopp et al., 2015), to an immature diplodocid (Woodruff and Fowler, 2012). Some studies recognize *Suuwassea* as a valid genus and interpret the holotype as non-juvenile (Wedel and Taylor, 2013; Hedrick et al., 2014).

Woodruff and Fowler (2012) interpreted the following morphologic traits as being ontogenetically influenced: narrow spine bifurcation, anterior prominence at the dentary symphysis (a "chin"), curvature of the tooth row, decreased vertebral pneumaticity, postparietal "foramen", unfused scapulocoracoid (yet note the issues regarding fusion), and elongate pedal phalanges. Woodruff and Fowler (2012) stated that until a histologic analysis is performed, the ontogenetic status *Suuwassea* would not be definitive. Hedrick et al. (2014) examined the histology of *Suuwassea*, and from analy-

sis of the holotype tibia, they conclude that *Suuwassea* is HOS 8-9 out of 13 (however it is important to note that the HOS was constructed primarily using femora, thus tibiae may not correspond 1:1). However from this HOS designation, Hedrick et al. (2014) inferred that *Suuwassea* (ANS 21122) was nearly skeletally mature, had reached sexual maturity, was a valid genus, and that the plesiomorphic characters were not related to immaturity. While we applaud Hedrick et al. (2014) in conducting a histologic analysis to examine life history information, comparison with a specimen exhibiting similar morphologies (MOR 592) suggests an alternative taxonomic interpretation (Figure 17).

The *Diplodocus* sp. MOR 592 displays the same plesiomorphic characters observed in *Suuwassea* (see above). Originally referred to as *Amphicoelias* on the basis of a "stovepipe" femur (Wilson and Smith, 1996), and subsequently considered a possible new genus, this specimen has since been alternatively recognized as an immature *Diplodocus* sp. (Woodruff and Fowler, 2012; Woodruff and Foster, 2014; however note that Whitlock and Harris, 2010 consider it a dicraeosaurid). Aside from the plesiomorphic characters, MOR 592 also has a similar femur length (124.5 cm versus the calculated 135 cm of *Suuwassea* [Hedrick et al., 2014]). Likewise thin-sectioning of the MOR 592 femur indicates that it is HOS 9 out of 13. Furthermore, thin-sectioning of a dorsal rib of MOR 592 and ANS 21122 records a minimum of eight preserved LAGs in both specimens; and both lack an EFS in any elements histologically examined (Figure 17). Both specimens exhibit similar morphology, and both exhibit similar histology, supporting the hypothesis that they represent similar ontogenetic stages.

We would suggest that an alternative explanation for the plesiomorphic characters of MOR 592 is that it is an immature *Diplodocus* sp. (in agreement with Woodruff and Fowler, 2012) rather than a Laurasian dicraeosaurid (Whitlock and Harris, 2010). Likewise the abundance of shared features between MOR 592 and ANS 21122 support *Suuwassea* is an immature individual (Figure 17). While the similarities between MOR 592 and ANS 21122 may be attributable to their ontogenetic stage, the specific vertebral morphologies of *Suuwassea* resemble those of other immature apatosaurine individuals (such as CM 555 [*A. excelsus* or *Brontosaurus excelsus*] or CM 3390 [*Apatosaurus* sp.]), thus these apparent distinctions can be conversely interpreted as the variation observed in an immature animal of a known taxon. In consideration of the fact that morphological and histologic analyses by separate investigating parties (Woodruff and Fowler, 2012; Hedrick et al., 2014; this current analysis) have reached comparable ontogenetic results, we advocate that the taxonomic status of *Suuwassea* remains unresolved. We consider the morphology and histology to indicate that, rather than representing a distinct taxon, *Suuwassea emilieae* (ANS 21122) is more likely an immature *Apatosaurus*.

The issues discussed above regarding taxonomy should not be trivialized. While MOR 592 could certainly be an immature *Diplodocus* sp., *Suuwassea* at this time could equally represent an immature *Apatosaurus* sp., a distinct taxon, a more or less mature individual or taxon with pedomorphic attributes, and possibly a combination of these conditions. Currently the holotype material does not unanimously support one distinct interpretation. The greater importance in this ongoing discussion is that a specimen exists where alternative taxonomy is derived from differing morphologic interpretations. While the characters used in a phylogenetic analysis are derived from morphologic attributes, this analysis would suggest that many of the characters are ontogenetically dependent. As demonstrated with tyrannosaurs (Carr and Williamson, 2004; Fowler et al., 2011), ceratopsians (Scannella and Horner, 2010; Scannella et al., 2014; Frederickson and Tumarkin-Deratzian, 2014), and hadrosaurs (Campione et al., 2013; Fowler and Horner, 2015), ontogeny (and stratigraphy) does affect taxonomy (likewise echoed in Hone et al., 2016). In animals that undergo an order of magnitude in size change, one could predict that many phylogenetic characters are simultaneously size determinant (ontogenetic in the sense they change as an animal gets larger with age) characters. Such has previously been demonstrated where immature individuals of a derived taxon appear to occupy a more basal position (Campione et al., 2013; Carballido and Sander, 2014). While phylogeny will not be made or broken by a single character, some characters (such neural spine bifurcation or the postparietal aperture) have historically been important for taxonomic distinction (laudably Tschopp et al., 2015 noted the significance of such). The ontogenetic development of the postparietal aperture may appear minor, but the ontogenetic development of another cranial opening was one feature used to re-examine derived Triceratopsini taxonomy (Scannella

and Horner, 2010; which is, however, still under debate).

As this analysis calls for the combined efforts of morphologic and histologic observations to better understand ontogeny, perhaps future studies should look to stratigraphy, morphology, and histology as supportive information to enhance phylogenetic studies (such is already being done and is referred to as an ontogram; Frederickson and Tumarkin-Deratzian, 2014). Perhaps the true phylogeny of such conflicting specimens will be resolved from an ontogram-based inclusive approach.

Ontogenetic Compilation

In a like manner to the Nash Equilibrium Theory (Nash, 1950), the individual characters used in this H-MOS may seem insignificant or minor; but, by not forcefully competing (i.e., histologic characters trump morphological characters, or vice versa), each is an important contribution by itself while simultaneously supporting other characters. The design and simplicity of the H-MOS system is that it is not restricted to sauropods; as presented herein, this system has been tailored to a diplodocid series. But the importance and implication of histology and morphology are not restricted to sauropodomorphs. Therefore an H-MOS style system should be adopted and incorporated into all dinosaurian ontogeny studies. In this analysis, the outcome of such a methodology is greater ontogenetic resolution and the predictive capabilities to infer diplodocid maturational stages and conditions.

As an example, let us examine the immature *Diplodocus* sp. MOR 592. A histologic section of the 124.5 cm long femur identifies it as HOS 9. Morphologic examination shows that the posterior cervical vertebrae are at the initial stage of spine bifurcation, while the dorsal vertebrae exhibit spine bifurcation that is more similar to the adult morphology. CT scans of the vertebrae illustrate a thinning of the median septum and interspersed camellae and camerae within the condyle and cotyle. The calculated body mass is 3,205 kg. Histology of the dorsal ribs record a minimum of eight preserved LAGs with no evidence of an EFS. The combination of these characters helps to define our diplodocid H-MOS Stage 3. Instead of solely using HOS or degree of spine bifurcation to determine a relative maturational state, or dorsal rib data to determine a minimum age, the H-MOS method creates a larger depiction of the histological and morphological attributes of each size range, creating a better representation of the animal as a whole.

Potentially our outlined H-MOS method even has the capacity to be applied to fragmentary and isolated diplodocid elements. While the predictive capabilities based on a single element are less absolute than multi-element analysis, it nonetheless reinforces the notion that each piece of data is significant (i.e., even isolated elements are vital data points). Every specimen helps create a more accurate index. An isolated femur that can be sectioned will reveal HOS. HOS coupled with femur dimensions could contribute to the range (such as HOS range and calculated body mass) of the particular growth stage. Similarly, on an isolated cervical vertebra, the degree of spine bifurcation and pneumaticity can be noted, and the neural spine could be sampled, while the entire vertebra could be CT scanned. While more complete specimens contribute far more data, the H-MOS methodology illustrates that isolated elements should not be overlooked because these seemingly “unimportant” specimens still represent useful data.

As presented, the H-MOS method is in its infancy, and undoubtedly more specimens, characters, ontogenetic divisions, and finer stage resolution will be added to increase its accuracy. Most recently the Remodeling Stages of Mitchell et al. (2017) represent a new histologic consideration, and for certain this new histologic character will be incorporated into future H-MOS works. While this H-MOS seeks to illuminate the life histories of sauropods, some variables such as sexual maturity, ASP, and degrees of intraspecific variation as yet remain unresolved. Documentation in vertebrates shows that sexual maturity typically precedes skeletally maturity (van Tienhoven, 1983). If this holds true for the examined sauropods, perhaps some of the H-MOS Stage 3 specimens were already sexually mature (Griebeler et al., 2013; Waskow and Sander, 2014). Therefore determination of sexual maturity would be a valuable future H-MOS character.

A further factor to consider in any H-MOS style analysis – even the one described herein – are the effects of intraspecific and interspecific variation. Intraspecific variation exists in all species, and only large sample sets (like those demonstrated for *Triceratops* [100+; Scannella et al., 2014] and *Maiasaura* [50; Woodward et al., 2015]) will allow for interspecific variation to be recognized and accounted for. Even within the relatively small sample size of this analysis, the degree of intraspecific variation has likely gone unchecked, and could even be affecting our demarcations and maturational inferences. Furthermore, in this analysis we

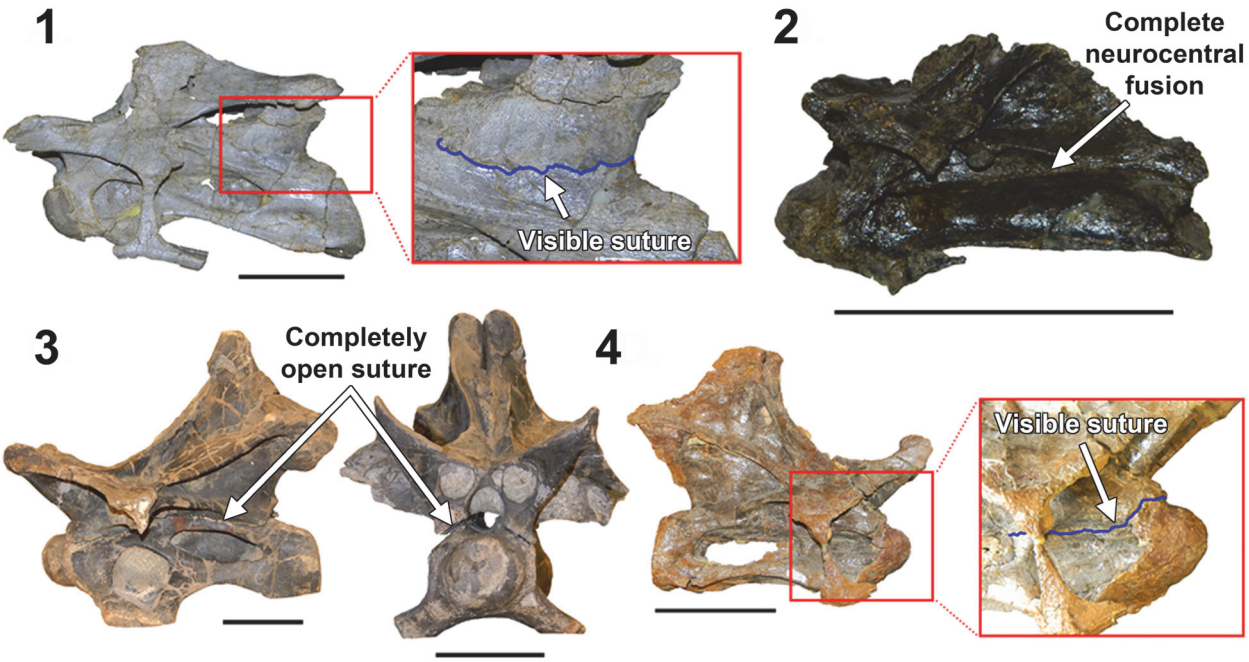

FIGURE 18. The degrees and variation of neurocentral fusion in diplodocid cervical vertebrae indicate that fusion is not uniformly indicative of maturity. **1,** The posteriorly unfused H-MOS Stage 2 *Diplodocus* sp. MOR 790 8-10-96-204; **2,** The completely fused H-MOS Stage 1 diplodocid indeterminate MOR 714 7-22-3-53; **3,** The completely unfused H-MOS Stage 3 *Apatosaurus excelsus* (or *Brontosaurus excelsus*) CM 555; **4,** The anteriorly unfused H-MOS Stage 3 *Diplodocus* sp. MOR 592. Red inset boxes highlight the visible sutures (in blue). Not to scale. Scale bar equals 10 cm.

make a collective ontogenetic trajectory for *Diplodocus*, yet our dataset is comprised of known and unknown species. In all likelihood, interspecific variation did exist amongst species of the same genus, and as addressed before, not accounting for these factors could weaken said system. The reason for such inclusion is twofold: 1) we unfortunately do not have enough specimens of precisely known taxonomy at this time to make a *Diplodocus* species-level H-MOS, and 2) the goal of initial, preliminary analyses such as this are to first recognize patterns. Initial ontogenetic studies of *Triceratops* cranial ornamentation noted general patterns such as orbital horn curvature and morphology of epoccipitals (Horner and Goodwin, 2006). And building upon this, subsequent analyses noted that some specimens or features that did not universally conform could be explained as ontogimorphs via anagenesis from *T. horridus* to *T. prorsus* (Scannella et al., 2014). In like manner, aspects of the presented H-MOS could later be determined to be affected by variation, or they could represent signals worthy of future exanimation. Undoubtedly future analyses will find flaws in this initial system, but the initial patterns we present serve as the platform for subsequent works.

Additionally, further examinations may reveal the validity/invalidity of previously used maturational features. Throughout this current analysis, one may have noted the absence of two popular sauropod maturational characters: neurocentral fusion and Elongation Index. Brochu (1996, 1999), Irmis (2007) and Ikejiri (2012) have demonstrated that crocodilians can have drastically delayed or even a complete lack of vertebral fusion within presacral vertebrae, while Bailleul et al. (2016) demonstrated similar findings in cranial sutures. In all the diplodocids we examined, there was no consistency or pattern to vertebral fusion (Figure 18). In a cervical approximately 10 cm long there can be complete neurocentral fusion, whereas in larger cervicals (~ 25 to 30 cm) fusion can range from completely open to fusing only in the anterior portion or only in the posterior region of the neural arch (Figure 18). As Brochu (1996, 1999), Irmis (2007), Ikejiri (2012), and Bailleul et al. (2016) demonstrated, while sutural patterns may be evident in some crocodilians, (neurocentral) fusion in dinosaurs appears to be sporadic and should only be used with caution when inferring maturity. Conversely, Melstrom et al. (2016) note a pattern in sacral fusion and open dorsal sutures in an imma-

ture *Barosaurus*, and therefore conclude that neurocentral fusion could be a reliable indicator of maturity. Such complete vertebral series will be the way to document such, and perhaps a general fusion pattern exists, but that deviation from said pattern has high plasticity (this could explain the degrees of fusion observed in this study).

The other excluded assessment is that of Elongation Index (EI). Defined as the ratio between the length of the centrum (condyle to cotyle length) divided by the cotyle diameter (cotyle width; Wedel et al., 2000), it has been inferred that EI values might be taxonomically or maturationally specific (Wedel and Taylor, 2013). A simple calculation of EI for 12 diplodocid cervical series indicates that taxonomically, serially, ontogenetically, and individually, EI is extremely variable (see Appendices 5-8). However, if the EI trends among these diplodocids are legitimate, this suggests that higher EI values collectively could be more indicative of an immature condition (note that this would support the findings of Woodruff and Fowler [2012] that juvenile diplodocid vertebrae primarily increase vertebral length earlier in ontogeny, and later growth is principally directed at width – resulting in a high EI during early ontogeny, and a lower EI in later life). Yet since the nature of EI is so variable, and our understanding of the ontogenetic role of EI is still in its infancy, we would temporarily avoid individual vertebral EI as a means to infer maturity. While variation in neurocentral fusion and EI could easily be explainable and intraspecific variation, and such patterns or trends may be legitimate, at this time we do not possess the supportive data to suggest that these are reliable maturational indicators across ontogeny. It is important to note that Melstrom et al. (2016) note the distribution of EI within the partial *Barosaurus* vertebral series, and their findings support that it should be a character examined in future analyses.

Likewise, further analyses may indicate that some characters are more maturationally delineated than others (such as sexually maturity versus mass). As Hone et al. (2016) demonstrated, varied life history information only enhances ontogenetic resolution and maturational distinctions. Yet we must remember, that as stated most recently by Goodwin and Evans (2016), ontogeny is developmental progression, and not strictly developmental demarcations; and even though this analysis attempts to categorize sauropod ontogeny, in reality we should expect many of these developmental lines to be gradational.

An additional caution to the H-MOS system would be the recognition of skeletally mature, “small” animals. While it is outside of this study’s scope, the *Camarasaurus* SMA 0002 provides such a cautionary example. For an “average” body size, SMA 0002 is rather small (calculated mass of 10,634 kg), yet histologic examination by Waskow and Sander (2014) revealed that this specimen was approximately 40 years old at the time of death making it the oldest (and it is also the stratigraphically lowest) *Camarasaurus* sampled to date (SMA 0002 has an EFS, so theoretically H-MOS 4). Therefore, this specimen (or similar small-statured morphs) could give conflicting morphologic and histologic data. Many of the H-MOS characters appear to be correlated with some aspect of body size, so a smaller, mature animal could have some morphologies lesser expressed (and vice versa). While this current analysis has not identified such a specimen, we propose in the case where a specimen expressed such conflicting morphologies, this would serve as an “alert” to indicate something special about the animal’s life history. The degrees of intraspecific variation will likely affect interpretations but the recognition of variability will only strengthen our understanding of development.

Likewise sample size must be recognized as a factor towards predictive capabilities. The sample size of the Horner et al. (2000) analysis of *Maiasaura* growth dynamics was not statistically significant (n=six), yet the observed trends and hypotheses of that study served as a starting point and a “stepping stone” for the follow-up analysis of Woodward et al. (2015), which represents the largest single population dinosaur growth study (n=50); and this study confirmed the preliminary data of Horner et al. (2000).

Finally, it may certainly become necessary to have family, genera, or even species specific H-MOS tables (e.g., the body mass estimations of *Apatosaurus* do not ontogenetically correspond with *Diplodocus*, so an *Apatosaurus* mass range will need to be calculated). The argument could be presented that such a system (even this initial H-MOS) or further refined systems are not warranted because such do not uniformly apply, or would inherently be so complex. Single aspects of life history can be simply explained (e.g., HOS or MOS), yet the ultimate goal of the H-MOS is an attempt to better understand the life history of the dinosaur in question (as opposed to only diplodocids; i.e., “DOS”; for a good review of this topic, see Hone et al. [2016]). While the presented H-MOS demarcations do not apply ubiquitously to other sauropod

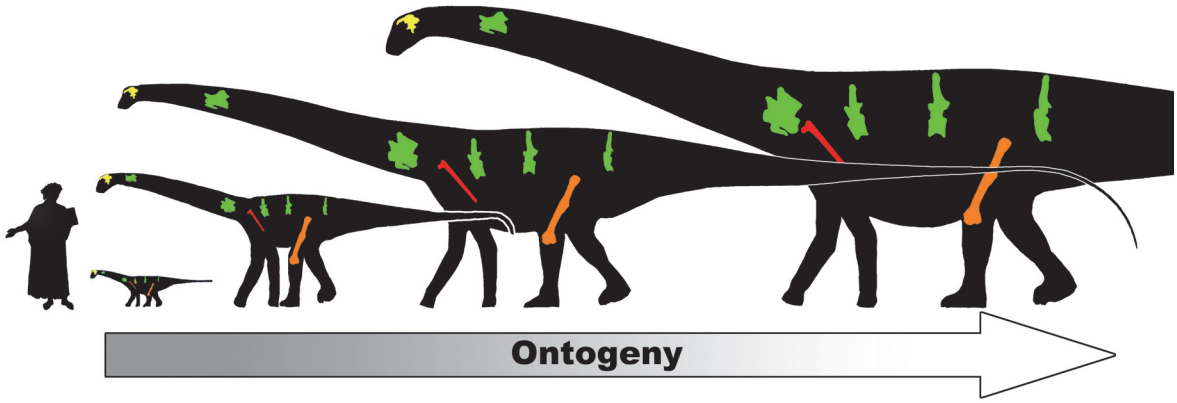

	H-MOS 1	H-MOS 2	H-MOS 3	H-MOS 4
Postparietal Aperture	NA	Present	Present	Absent
LAGs	<2	2 - 6	7 - 10	>20
Cervical Pneumaticity	Acamerate	Pro- to Camerate	Camerate	Camerate
Ant. Cerv. Bifurcation	None	None	Weakly	Fully
Pos. Cerv. Bifurcation	None	Weakly	Narrow	Fully
Dorsal Pneumaticity	NA	Acamerate	Camerate	Camerate
Ant. Dor. Bifurcation	None	Narrow	Narrow	Fully
Pos. Dor. Bifurcation	None	Narrow	Narrow	Fully
Ant. Caudal Bifurcation	None	None	None	Fully
Spine Trabeculae (mm)	NA	≤ 1	≥ 3	NA
HOS	<4	5 - 7	8 - 10	>10
Fem. Head Orientation	NA	20° - 11°	10° - 5°	<5°
4th Trochanter	Proximal	Proximal	Proximal to Mid.	Mid.
Fem. Length (mm)	<800	800 – 1,200	1,200 – 1,450	>1,450
Body Mass (kg)	<1,800	2,000 – 3,000	3,000 – 6,000	>6,000

FIGURE 19. An ontogenetic trajectory in consideration of morphologic and histologic attributes for the Morrison diplodocid *Diplodocus*. Note diplodocids, and possibly all other sauropods, did not skeletally develop along an isometric trajectory. Human scale bar is Dante Alighieri from Domenico di Michelino's "*La commedia illumina Firenze*", depicting Dante as 1.63 m tall. Modified silhouette of *Diplodocus carnegii* CM 84 by S. Hartman and available via PhyloPic under the Creative Commons Attribution-ShareAlike 3.0 Unported License.

clades (i.e., Macronaria), the methodology of this system can be incorporated throughout all of Sauropodomorpha, and in fact all of Dinosauria. By continually supplementing, adapting, modifying, and applying an H-MOS style system–and any future subsidiary systems–our resolution of life history only intensifies.

CONCLUSION

Whereas the recognition of a single feature's developmental trajectory is important, this analysis indicates that groups of changes are observed during sauropod ontogeny – i.e., individual features appear to substantiate one another in terms of inferred maturational states. The analysis of both morphologic and histologic attributes of multiple cranial and postcranial elements supports a correlation of maturational states through ontogeny. While the understanding of a single character's development is important, the recognition of a suite of defining histologic and morphologic characters allows for a better recognition of each maturational range. The proposed Histo-Morph Ontogeny Scale incorporates multiple variables and allows for a more complete picture of growth changes in these animals (Figure 19).

ACKNOWLEDGEMENTS

We would like to thank G. Ohrstrom and E. and J. Sands for their gracious and continuing support to the MOR Paleontology Department. Without the time and consideration of all the museum staff and collection managers, none of this work would have been possible. We humbly thank K. Siber and the entire staff and family of the Sauriermuseum Aathal; O. Wings and H. Mallison at the Museum für Naturkunde – Leibniz Research Institute for Evolution and Biodiversity; C. Mehling and M.

Norell at the American Museum of Natural History; A. Henrici, M. Lamanna, C. Beard, D. Berman, and D. Pickering of the Carnegie Museum of Natural History; T. Daeschler and the Academy of Natural Sciences at Drexel University; S. Lucas and the New Mexico Museum of Natural History and Science; and M. Sander, K. Waskow, N. Klein, and DFG Research Unit 533 from the Steinmann Institut für Geologie, Paläontologie und Mineralogie. K. Ugrin and the staff of Advanced Medical Imaging at Bozeman Deaconess Hospital generously donated their time and use of their CT scanner. H. Woodward and D. Varricchio provided invaluable insight and assistance through manuscript revision and preparation. Further we would like to thank H.D. Sues, E. Tschopp, K. Waskow, R. Wilhite, J. Foster, M. Wedel, M. Taylor, B. Hedrick, J. Harris, E. Prondvai, K. Stein, K. Stevens, J. McIntosh, G. Storrs, J. Scannella, E. Freedman-Fowler, J. Wilson, K. Nordén, B. Baziak, S. Hartman, P. Raia, and two anonymous reviewers for expert advice and assistance, review, and continuing support throughout this project.

REFERENCES

Abramoff, M.D., Magalhaes, P.J., and Ram, S.J. 2004. Image Processing with ImageJ. *Biophotonics International,* 11(7):36-42.

Bailleul, A.M., Scannella, J.B., Horner, J.R., and Evans, D.C. 2016. Fusion patterns in the skulls of modern archosaurs reveal that sutures are ambiguous maturity indicators for the Dinosauria. *PLoS ONE,* 11(2):e0147687. doi:10.1371/journal.pone.0147687

Bakker, R.T. 1986. *The Dinosaur Heresies*. William Morrow and Company, New York.

Balanoff, A.M., Bever, G.S., and Ikejiri, T. 2010. The braincase of *Apatosaurus* (Dinosauria: Sauropoda) based on computed tomography of a new specimen with comments on variation and evolution in sauropod neuroanatomy. *American Museum Novitates*, 3677:1-32.

Berman, D.S. and McIntosh, J.S. 1978. Skull and relationships of the Upper Jurassic sauropod *Apatosaurus* (Reptilia, Saurischia). *Bulletin of the Carnegie Museum of Natural History,* 8:1-35.

Bonnan, M.F. 2004. Morphometric analysis of humerus and femur shape in Morrison sauropods: implications for functional morphology and paleobiology. *Paleobiology*, 30:444-470.

Borsuk-Bialynicka, M. 1977. A new camarasaurid sauropod *Opisthocoelicaudia skarzynskii*, gen. n., sp. n. from the Upper Cretaceous of Mongolia. *Acta Palaeontologia Polonica,* 37:1-64.

Brochu, C.A. 1996. Closure of neurocentral sutures during crocodilian ontogeny: implications for maturity assessment in fossil archosaurs. *Journal of Vertebrate Paleontology*, 16:49-62.

Brochu, C.A. 1999. Phylogeny, systematics, and historical biogeography of Alligatoroidea. *Society of Vertebrate Paleontology Memoir,* 6:9-100.

Campione, N.E., Brink, K.S., Freedman, E.A., McGarrity, C.T., and Evans, D.C. 2013. '*Glishades ericksoni*', an indeterminate juvenile hadrosaurid from the Two Medicine Formation of Montana: implications for hadrosauroid diversity in the latest Cretaceous (Campanian-Maastrichtian) of western North America. *Palaeobiodiversity and Palaeoenvironments*, 93:65-75.

Campione, N.E. and Evans, D.C. 2011. Cranial growth and variation in edmontosaurs (Dinosauria: Hadrosauridae): implications for latest Cretaceous megaherbivore diversity in North America. *PLoS One*, 6(9):e25186.

Campione, N.E. and Evans, D.C. 2012. A universal scaling relationship between body mass and proximal limb bone dimensions in quadrupedal terrestrial tetrapods. *BMC Biology*, 10:60.

Carballido, J.L., Marpmann, J.S., Schwarz-Wings, D., and Pabst, B. 2012. New information on a juvenile sauropod specimen from the Morrison Formation and the reassessment of its systematic position. *Palaeontology*, 55:567-582.

Carballido, J.L. and Sander, P.M. 2014. Postcranial axial skeleton of *Europasaurus holgeri* (Dinosauria, Sauropoda) from the Upper Jurassic of Germany: implications for sauropod ontogeny and phylogenetic relationships of basal Macronaria. *Journal of Systematic Palaeontology*, 12:335-387.

Carpenter, K. 2013. History, sedimentology, and taphonomy of the Carnegie Quarry, Dinosaur National Monument, Utah. *Annals of Carnegie Museum*, 81(3):153-232.

Carr, T.D. 1999. Craniofacial ontogeny in tyrannosauridae (Dinosauria, Coelurosauria). *Journal of Vertebrate Paleontology*, 19:497-520.

Carr, T.D. and Williamson, T.E. 2004. Diversity of late Maastrichtian Tyrannosauridae (Dinosauria: Theropoda) from western North America. *Zoological Journal of the Linnean Society*, 142:479-523.

Case, T.J. 1978. Speculations on the growth rate and reproduction of some dinosaurs. *Paleobiology*, 4:320-328.

Castanet, J., Francillon-Vieillot, H., Meunier, F.J., and de Ricqlès, A. 1992. Bone and Individual aging, p. 245-283. In Hall, B.K. (ed.), *Bone: A Treatise Volume*. CRC Press, London.

Christian, A. 2002. Neck posture and overall body design in sauropods. *Mitt Museum Naturkunde Berlin Geowissenschaftl Reihe,* 5:271-281.

Curry, K.A. 1999. Ontogenetic histology of *Apatosaurus* (Dinosauria: Sauropoda): new insights on growth rates and longevity. *Journal of Vertebrate Paleontology*, 19:654-665.

de Ricqlès, A., Meunier, F.J., Castanet, J., and Francillon-Vieillot, H. 1991. Comparative microstructure of bone. *Bone,* 3:1-78.

Dodson, P. 1975. Taxonomic implications of relative growth in lambeosaurine hadrosaurs. *Systematic Biology*, 24:37-54.

Dodson, P. and Harris, J.D. 2001. Necks of sauropod dinosaurs: support of a nuchal ligament? *Journal of Morphology*, 248(3):224.

Erickson, G.M. 2005. Assessing dinosaur growth patterns: a microscopic revolution. *Trends in Ecology and Evolution*, 20: 677-684.

Erickson, G.M., Rogers, K.C., and Yerby, S.A. 2001. Dinosaurian growth patterns and rapid avian growth rates. *Nature*, 412:429-433.

Evans, D.C., Forster, C.A., and Reisz, R.R. 2005. The type specimen of *Tetragonosaurus erectofrons* (Ornithischia: Hadrosauridae) and the identification of juvenile Lambeosaurines, p. 349-366. In Currie, P.J. and Koppelhaus, E.B. (eds.), *Dinosaur Provincial Park*. Indiana University Press, Bloomington.

Fowler, E.A.F. and Horner, J.R. 2015. A new brachylophosaurin hadrosaur (Dinosauria: Ornithischia) with an intermediate nasal crest from the Campanian Judith River Formation of northcentral Montana. *PloS ONE*, 10(11):e0141304.

Fowler, D.W., Woodward, H.N., Freedman, E.A., Larson, P.L., and Horner, J.R. 2011. Reanalysis of "*Raptorex kriegsteini*": a juvenile tyrannosaurid dinosaur from Mongolia. *PLoS One*, 6(6):e21376.

Francillon-Vieillot, H., de Buffrénil, V., Castanet, J., Géraudie, J., Meunier, F.J., Sire, J.Y., Zylberberg, L., and de Ricqlès, A. 1990. Microstructure and mineralization of vertebrate skeletal tissues, p. 175-234. In Carter, J.G. (ed.), *Skeletal Biomineralization: Patterns, Processes and Evolutionary Trends*. Van Nostrand Reinhold, New York.

Frederickson, J.A. and Tumarkin-Deratzian, A.R. 2014. Craniofacial ontogeny in *Centrosaurus apertus*. *PeerJ*, 2:e252.

Gallina, P.A. 2011. Notes on the axial skeleton of the titanosaur *Bonitasaura salgadoi* (Dinosauria-Sauropoda). *Anais Da Academia Brasileira de Ciências,* 83:235-246.

Gallina, P.A. 2012. Histología ósea del titanosaurio *Bonitasaura salgadoi* (Dinosauria: Sauropoda) del Cretácico Superior de Patagonia. *Ameghiniana,* 49:289302.

Gilmore, C.W. 1925. A nearly complete articulated skeleton of *Camarasaurus*, a saurischian dinosaur from the Dinosaur National Monument, Utah. *Memoirs of the Carnegie Museum*, 10:347-384.

Gilmore, C.W. 1936. Osteology of *Apatosaurus* with special reference to specimens in the Carnegie Museum. *Memoirs of the Carnegie Museum*, 11:175-300.

Goodwin, M.B. and Evans, D.C. 2016. The early expression of squamosal horns and parietal ornamentation confirmed by new end-stage juvenile *Pachycephalosaurus* fossils from the Upper Cretaceous Hell Creek Formation, Montana. *Journal of Vertebrate Paleontology*, e1078343.

Grey, H. 1858. *Anatomy: Descriptive and Surgical.* Parker and Son, London.

Griebeler, E.M., Klein, N., and Sander, P.M. 2013. Aging, maturation and growth of sauropodomorph dinosaurs as deduced from growth curves using long bone histological data: An assessment of methodological constraints and solutions. *PLoS ONE*, 8(6):e67012.

Harris, J.D. 2006a. Cranial osteology of *Suuwassea emilieae* (Sauropoda: Diplodocoidea: Flagellicaudata) from the Upper Jurassic Morrison Formation of Montana, USA. *Journal of Vertebrate Paleontology*, 26:88-102.

Harris, J.D. 2006b. The significance of *Suuwassea emilieae* (Dinosauria: Sauropoda) for flagellicaudatan intrarelationships and evolution. *Journal of Systematic Palaeontology*, 4:185-198.

Harris, J.D. and Dodson, P. 2004. A new diplodocoid sauropod dinosaur from the Upper Jurassic Morrison Formation of Montana, USA. *Acta Palaeontologica Polonica*, 49:197-210.

Hatcher, J.B. 1901. *Diplodocus* Marsh: its osteology, taxonomy, and probable habits, with a restoration of the skeleton. *Memoirs of the Carnegie Museum*, 1:1-63.

Hatcher, J.B. 1903. Osteology of *Haplocanthosaurus* with additional remarks on *Diplodocus*. *Memoirs of the Carnegie Museum*, 1:1-75.

Hedrick, B.P., Tumarkin-Deratzian, A.R., and Dodson, P. 2014. Bone microstructure and relative age of the holotype specimen of the diplodocoid sauropod dinosaur *Suuwassea emilieae*. *Acta Palaeontologica Polonica*, 59:295-304.

Holland, W.J. 1924. The skull of *Diplodocus*. *Memoirs of the Carnegie Museum*, 9:379-403.

Hone, D.W.E., Farke, A.A., and Wedel, M.J. 2016. Ontogeny and the fossil record: What, if anything, is an adult dinosaur? *Biology Letters*, 12:20150947.

Hopson, J.A. 1975. The evolution of cranial display structures in hadrosaurian dinosaurs. *Paleobiology*, 1:21-43.

Hopson, J.A. 1979. Paleoneurology, p. 39-146. In Gans, C., Northcutt, R.C., and Ulinski, P. (eds.), *Biology of the Reptilia Volume 9 Neurology A*. Academic Press, London.

Horner, J.R., de Ricqlès, A., and Padian, K. 1999. Variation in dinosaur skeletochronology indicators: implications for age assessment and physiology. *Paleobiology*, 25(3):295-304.

Horner, J.R., de Ricqlès, A., and Padian, K. 2000. Long bone histology of the hadrosaurid dinosaur *Maiasaura peeblesorum*: growth dynamics and physiology based on an ontogenetic series of skeletal elements. *Journal of Vertebrate Paleontology*, 20:115-129.

Horner, J.R. and Goodwin, M.B. 2006. Major cranial changes during *Triceratops* ontogeny. *Proceedings of the Royal Society B: Biological Sciences*, 273:2757-2761.

Horner, J.R. and Goodwin, M.B. 2009. Extreme cranial ontogeny in the Upper Cretaceous dinosaur *Pachycephalosaurus*. *PLoS One*, 4:e7626.

Horner, J.R., Goodwin, M.B., and Myhrvold, N. 2011. Dinosaur census reveals abundant *Tyrannosaurus* and rare ontogenetic stages in the Upper Cretaceous Hell Creek Formation (Maastrichtian), Montana, USA. *PloS One*, 6(2):e16574.

Horner, J.R. and Padian, K. 2004. Age and growth dynamics of *Tyrannosaurus rex*. *Proceedings of the Royal Society of London. Series B: Biological Sciences*, 271:1875-1880.

Huttenlocker, A.K., Woodward, H.N., and Hall, B.K. 2013. The biology of bone, p. 13-34. In Padian, K. and Lamm, E.T. (eds.), *Bone Histology of Fossil Tetrapods: Advancing Methods, Analysis, and Interpretation.* University of California Press, Berkeley.

Ikejiri, T. 2012. Histology?based morphology of the neurocentral synchondrosis in *Alligator mississippiensis (Archosauria, Crocodylia)*. The Anatomical Record, 295:18-31.

Ikejiri, T., Tidwell, V., and Trexler, D.L. 2005. New adult specimens of *Camarasaurus lentus* highlight ontogenetic variation within the species, p. 154-179. In Tidwell, V. and Carpenter, K. (eds.), *Thunder-lizards: The Sauropodomorph Dinosaurs*. Indiana University Press, Bloomington.

Irmis, R.B. 2007. Axial skeleton ontogeny in the Parasuchia (Archosauria: Pseudosuchia) and its implications for ontogenetic determination in archosaurs. *Journal of Vertebrate Paleontology*, 27:350-361.

Janensch, W. 1929. Die Wirbelsaule der Gattung *Dicraeosaurus*. *Palaeontographica*, 2:1-34.

Klein, N. and Sander, M. 2008. Ontogenetic stages in the long bone histology of sauropod dinosaurs. *Paleobiology*, 34:247-263.

Knoll, F., Witmer, L.M., Ortega, F., Ridgely, R.C., and Schwarz-Wings, D. 2012. The braincase of the basal sauropod dinosaur *Spinophorosaurus* and 3D reconstructions of the cranial endocast and inner ear. *PloS One*, 7(1):e30060.

Lee, A.H. and Werning, S. 2008. Sexual maturity in growing dinosaurs does not fit reptilian growth models. *Proceedings of the National Academy of Sciences*, 105(2):582-587.

Lehman, T.M. and Woodward, H.N. 2008. Modelling growth rates for sauropod dinosaurs. *Paleobiology*, 34:264-281.

Lovelace, D.M., Hartman, S.A., and Wahl, W.R. 2007. Morphology of a specimen of *Supersaurus* (Dinosauria, Sauropoda) from the Morrison Formation of Wyoming, and a re-evaluation of diplodocid phylogeny. *Arquivos do Museu Nacional, Rio de Janeiro*, 65:527-544.

Lull, R.S. 1919. The sauropod dinosaur *Barosaurus* Marsh: redescription of the type specimens in the Peabody Museum, Yale University. *Connecticut Academy of Arts and Sciences,* 6:1-42.

Mannion, P.D., Upchurch, P., Mateus, O., Barnes, R.N., and Jones, M.E. 2012. New information on the anatomy and systematic position of *Dinheirosaurus lourinhanensis* (Sauropoda: Diplodocoidea) from the Late Jurassic of Portugal, with a review of European diplodocoids. *Journal of Systematic Palaeontology*, 10:521-551.

Mazzetta, G.V., Christiansen, P., and Farina, R.A. 2004. Giants and bizarres: body size of some southern South American Cretaceous dinosaurs. *Historical Biology*, 16(2-4):71-83.

McIntosh, J.S. 1981. Annotated catalogue of the dinosaurs (Reptilia, Archosauria) in the collections of Carnegie Museum of Natural History. *Bulletin of the Carnegie Museum of Natural History,* 18:1-67.

McIntosh, J.S. 1990. Species determination in sauropod dinosaurs with tentative suggestions for their classification, p. 53-69. Carpenter, K. and Currie, P.J. (eds.), *Dinosaur Systematics: Approaches and Perspectives*. Cambridge University Press.

McIntosh, J.S. 2005. The genus *Barosaurus* Marsh (Sauropoda, Diplodocidae), p. 38-77. In Tidwell, V. and Carpenter, K. (eds.), *Thunder-Lizards*: *The Sauropodomorph Dinosaurs*: Indiana University Press, Bloomington.

McIntosh, J.S., Miles, C.A., Cloward, K.C., and Parker, J.R. 1996. A new nearly complete skeleton of *Camarasaurus*. *Bulletin of the Gunma Museum of Natural History*, 1-87.

McIntosh, J.S. and Williams, M.E. 1988. A new species of sauropod dinosaur, *Haplocanthosaurus delfsi* sp. nov., from the Upper Jurassic Morrison Fm. of Colorado. *Kirtlandia*, 43:3-26.

Melstrom, K.M., D'emic, M.D., Chure, D., and Wilson, J.A. 2016. A juvenile sauropod dinosaur from the Late Jurassic of Utah, U.S.A., presents further evidence of an avian style air-sac system. *Journal of Vertebrate Paleontology* (advance online publication). DOI:10.1080/02724634.2016.1111898

Michelis, I. 2004. *Taphonomie des Howe Quarry's (Morrison-Formation, Oberer Jura), Bighorn County, Wyoming, USA*. Unpublished PhD Thesis, Institute of Palaeontology, University of Bonn, Germany.

Mitchell, J., Sander, P.M., and Stein, K. 2017. Can secondary osteons be used as ontogenetic indicators in sauropods? Extending the histological ontogenetic stages into senescence. *Paleobiology*, 43: 1-22.

Mook, C.C. 1917. The fore and hind limbs of *Diplodocus*. *Bulletin of the American Museum of Natural History,* 37:815-819.

Myers, T.S. 2004. *Taphonomy of the Mother's Day Quarry: Implications for Gregarious Behavior in Sauropod Dinosaurs*. Unpublished PhD dissertation, University of Cincinnati, Cincinnati, Ohio, USA.

Myhrvold, N.P. 2013. Revisiting the estimation of dinosaur growth rates. *PLoS One,* 8(12):e81917.

Nash, J.F. 1950. Equilibrium points in n-person games. *Proceedings of the National Academy of Sciences*, 36:48-9.

Ostrom, J.H. and McIntosh, J.S. 1966. *Marsh's Dinosaurs*. Yale University Press, New Haven and London.

Otero, A., Gallina, P.A., Canale, J.I., and Haluza, A. 2012. Sauropod haemal arches: morphotypes, new classification and phylogenetic aspects. *Historical Biology*, 24:243-256.

Padian, K., de Ricqlès, A.J., and Horner, J.R. 2001. Dinosaurian growth rates and bird origins. *Nature*, 412(6845):405-408.

Padian, K. and Lamm, E.T. (eds.) 2013. *Bone Histology of Fossil Tetrapods: Advancing Methods, Analysis, and Interpretation*. University of California Press, Berkeley.

Remes, K. 2009. Taxonomy of Late Jurassic diplodocid sauropods from Tendaguru (Tanzania). *Fossil Record*, 12:23-46.

Rogers, K.C. and Erickson, G.M. 2005. Sauropod histology, p. 303-326. In Curry Rogers, C. and Wilson, J.A. (eds), *The Sauropods, Evolution and Paleobiology*. University of California Press, Berkeley, California.

Rogers, K.C., Whitney, M., D'Emic, M., and Bagley, B. 2016. Precocity in a tiny titanosaur from the Cretaceous of Madagascar. *Science*, 352(6284):450-453.

Salgado, L. 1999. The macroevolution of the Diplodocimorpha (Dinosauria; Sauropoda): a developmental model. *Ameghiniana*, 36:203-216.

Salgado, L. and Bonaparte, J.F. 1991. Un nuevo sauropodo Dicraeosauridae, *Amargasaurus cazaui* gen. et sp. nov., de la Formacion La Amarga, Neocomiano de la provincia del Neuquen, Argentina. *Ameghiniana*, 28:333-346.

Sampson, S.D., Ryan, M.J., and Tanke, D.H. 1997. Craniofacial ontogeny in centrosaurine dinosaurs (Ornithischia: Ceratopsidae): taxonomic and behavioral implications. *Zoological Journal of the Linnean Society,* 121:293-337.

Sander, P.M. 1999. Life history of Tendaguru sauropods as inferred from long bone histology. *Fossil Record*, 2(1):103-112.

Sander, P.M. 2000. Longbone histology of the Tendaguru sauropods: implications for growth and biology. *Paleobiology,* 26(3):466-488.

Sander, P.M., Klein, N., Buffetaut, E., Cuny, G., Suteethorn, V., and Le Loeuff, J. 2004. Adaptive radiation in sauropod dinosaurs: bone histology indicates rapid evolution of giant body size through acceleration. *Organisms Diversity and Evolution*, 4:165-173.

Sander, P.M. and Tückmantel, C. 2003. Bone lamina thickness, bone apposition rates, and age estimates in sauropod humeri and femora. *Palaontologische Zeitschrift*, 77:161-172.

Scannella, J.B., Fowler, D.W., Goodwin, M.B., and Horner, J.R. 2014. Evolutionary trends in *Triceratops* from the Hell Creek Formation, Montana. *Proceedings of the National Academy of Sciences*, 111:10245-10250.

Scannella, J.B. and Horner, J.R. 2010. *Torosaurus* Marsh, 1891, is *Triceratops* Marsh, 1889 (Ceratopsidae: Chasmosaurinae): synonymy through ontogeny. *Journal of Vertebrate Paleontology*, 30:1157-1168.

Schwarz, D., Frey, E., and Meyer, C.A. 2007a. Pneumaticity and soft-tissue reconstructions in the neck of diplodocid and dicraeosaurid sauropods. *Acta Palaeontologica Polonica*, 52(1):167.

Schwarz, D. and Fritsch, G. 2006. Pneumatic structures in the cervical vertebrae of the Late Jurassic Tendaguru sauropods Brachiosaurus brancai and Dicraeosaurus. *Eclogae Geologicae Helvetiae*, 99:65-78.

Schwarz, D., Ikejiri, T., Breithaupt, B.H., Sander, P.M., and Klein, N. 2007b. A nearly complete skeleton of an early juvenile diplodocid (Dinosauria: Sauropoda) from the lower Morrison formation (Late Jurassic) of North Central Wyoming and its implications for early ontogeny and pneumaticity in sauropods. *Historical Biology,* 19:225-253.

Schwarz-Wings, D. 2009. Reconstruction of the thoracic epaxial musculature of diplodocid and dicraeosaurid sauropods. *Journal of Vertebrate Paleontology,* 29:517-534.

Schwarz-Wings, D. and Frey, E. 2008. Is there an option for a pneumatic stabilization of sauropod necks? — an experimental and anatomical approach. *Palaeontologia Electronica,* 11:1-26.

Senter, P. 2007. Necks for sex: sexual selection as an explanation for sauropod dinosaur neck elongation. *Journal of Zoology,* 271:45-53.

Seymour, R.S. 2009. Raising the sauropod neck: it costs more to get less. *Biology Letters,* 5:317-319.

Stein, K. and Sander, M. 2009. Histological core drilling: a less destructive method for studying bone histology, p. 69-80. In Brown, M.A., Kane, J.F., and Parker, W.G. (eds.), *Methods In Fossil Preparation: Proceedings of the First Annual Fossil Preparation and Collections Symposium*.

Stevens, K.A. and Parrish, J.M. 1999. Neck posture and feeding habits of two Jurassic sauropod dinosaurs. *Science,* 284:798-800.

Stevens, K.A. and Parrish, M.J. 2005a. Digital reconstructions of sauropod dinosaurs and implications for feeding, p. 178-200. In Curry Rogers, K. and Wilson, J.A. (eds.), *The Sauropods, Evolution and Paleobiology.* University of California Press, Berkeley, California.

Stevens, K.A., and Parrish, J.M. 2005b. Neck posture, dentition and feeding strategies in Jurassic sauropod dinosaurs, p. 212-232. In Tidwell, V. and Carpenter, K. (eds.), *Thunder-lizards: The Sauropodomorph Dinosaurs*. Indiana University Press, Bloomington, Indiana.

Storrs, G.W., Oser, S.E., and Aull, M. 2012. Further analysis of a Late Jurassic dinosaur bone-bed from the Morrison Formation of Montana, USA, with a computed three-dimensional reconstruction. *Earth and Environmental Science Transactions of the Royal Society of Edinburgh*, 103(3-4):443-458.

Taylor, M.P., Wedel, M.J., and Naish, D. 2009. Head and neck posture in sauropod dinosaurs inferred from extant animals. *Acta Palaeontologica Polonica,* 54:213-220.

Thompson, D'A.W. 1942. *On Growth and Form, 2nd ed*. Cambridge University Press, Cambridge, UK.

Tschopp, E. and Mateus, O. 2013. The skull and neck of a new flagellicaudatan sauropod from the Morrison Formation and its implication for the evolution and ontogeny of diplodocid dinosaurs. *Journal of Systematic Palaeontology*, 11:1-36.

Tschopp, E., Mateus, O.V., and Benson, R.B.J. 2015. A specimen-level phylogenetic analysis and taxonomic revision of Diplodocidae (Dinosauria, Sauropoda). *PeerJ,* 3:e857.

Tsuihiji, T. 2004. The ligament system in the neck of *Rhea americana* and its implication for the bifurcated neural spines of sauropod dinosaurs. *Journal of Vertebrate Paleontology,* 24:165-172.

Tsuihiji, T., Watabe, M., Tsogtbaatar, K., Tsubamoto, T., Barsbold, R., Suzuki, S., Lee, A.H., Ridgely, R.C., Kawahara, Y., and Witmer, L.M. 2011. Cranial osteology of a juvenile specimen of *Tarbosaurus bataar* (Theropoda, Tyrannosauridae) from the Nemegt Formation (Upper Cretaceous) of Bugin Tsav, Mongolia. *Journal of Vertebrate Paleontology,* 31:497-517.

Turner, C.E. and Peterson, F. 1999. Biostratigraphy of dinosaurs in the upper Jurassic Morrison Formation of the western interior, USA, p. 77-114. In Gillette, D.D. (ed.), *Vertebrate paleontology in Utah*. Utah Geological Survey Miscellaneous Publication, Salt Lake City, Utah.

Upchurch, P., Barrett, P.M., and Dodson, P. 2004a. Sauropoda, p. 259–322. In Weishampel, D.B., Dodson, P., and Osmolska, H. (eds.), *The Dinosauria. Second edition*. University of California Press, Berkeley, California.

Upchurch, P., Tomida, Y., and Barrett, P.M. 2004b. A new specimen of *Apatosaurus ajax* (Sauropoda: Diplodocidae) from the Morrison Formation (Upper Jurassic) of Wyoming, USA. *National Science Museum Monographs*, 26:1-118.

van Tienhoven, A. 1983. *Reproductive Physiology of Vertebrates*. Cornell University Press, London.

Waskow, K. and Sander, P.M. 2014. Growth record and histological variation in the dorsal ribs of *Camarasaurus* sp. (Sauropoda). *Journal of Vertebrate Paleontology*, 34:852-869.

Waskow, K. and Mateus O. 2017. Dorsal rib histology of dinosaurs and a crocodile from western Portugal: Skeletochronological implications on age determination and life history traits. Comptes Rendus Palevol (advance online publication) doi: http://doi.org/10.1016/j.crpv.2017.01.003

Wedel, M.J., Cifelli, R.L., and Sanders, R.K. 2000. Osteology, paleobiology, and relationships of the sauropod dinosaur *Sauroposeidon*. *Acta Palaeontologica Polonica*, 45:343-388.

Wedel, M.J. 2003. The evolution of vertebral pneumaticity in sauropod dinosaurs. *Journal of Vertebrate Paleontology*, 23:344-357.

Wedel, M.J. 2005. Postcranial skeletal pneumaticity in sauropods and its implications for mass estimates, p. 201-228. In Curry Rogers, K. and Wilson, J.A. (eds.), *The Sauropods: Evolution and Paleobiology*. University of California Press, Berkeley, California.

Wedel, M.J. 2009. Evidence for bird-like air sacs in saurischian dinosaurs. *Journal of Experimental Zoology A,* 311:1-18.

Wedel, M.J. and Taylor, M.P. 2013. Neural spine bifurcation in sauropod dinosaurs of the Morrison Formation: ontogenetic and phylogenetic implications. *Palarch's Journal of Vertebrate Palaeontology*, 10(1):1-34.

Whitlock, J.A. 2011a. A phylogenetic analysis of Diplodocoidea (Saurischia: Sauropoda). *Zoological Journal of the Linnean Society*, 161:872-915.

Whitlock, J.A. 2011b. Inferences of diplodocoid (Sauropoda: Dinosauria) feeding behavior from snout shape and microwear analyses. *PLoS One*, 6(4):e18304.

Whitlock, J.A. and Harris, J.D. 2010. The dentary of *Suuwassea emilieae* (Sauropoda: Diplodocoidea). *Journal of Vertebrate Paleontology*, 30:1637-1641.

Whitlock, J.A., Wilson, J.A., and Lamanna, M.C. 2010. Description of a nearly complete juvenile skull of *Diplodocus* (Sauropoda: Diplodocoidea) from the Late Jurassic of North America. *Journal of Vertebrate Paleontology*, 30:442-457.

Wilson, J.A. and Smith, M. 1996. New remains of *Amphicoelias* Cope (Dinosauria: Sauropoda) from the Upper Jurassic of Montana and diplodocoid phylogeny. *Journal of Vertebrate Paleontology*, 16(Suppl. 3):73A.

Wilhite, R. 1999. *Ontogenetic variation in the appendicular skeleton of the genus Camarasaurus*. Master Thesis, Brigham Young University, Provo, Utah, USA.

Wilhite, R. 2003. *Biomechanical reconstruction of the appendicular skeleton in three North American Jurassic sauropods.* PhD Thesis, Louisiana State University, Baton Rouge, Louisiana, USA.

Wilhite, R. and Curtice, B. 1998. Ontogenetic variation in sauropod dinosaurs. *Journal of Vertebrate Paleontology,* 18(Suppl. 3):86A.

Woodruff, D.C. 2014. The anatomy of the bifurcated neural spine and its occurrence within Tetrapoda. *Journal of Morphology*, 275:1053-1065.

Woodruff, D.C. 2016. Nuchal ligament reconstructions in diplodocid sauropods support horizontal neck feeding postures. *Historical Biology* (advance online publication). DOI:10.1080/08912963.2016.1158257

Woodruff, D.C. and Foster, J.R. 2014. The fragile legacy of *Amphicoelias fragillimus* (Dinosauria: Sauropoda; Morrison Formation–latest Jurassic). *Volumina Jurassica*, 12(2):211-220.

Woodruff, D.C. and Foster, J.R. 2017. The first specimen of *Camarasaurus* (Dinosauria: Sauropoda) From Montana: The northernmost occurrence of the genus. *PLoS ONE,* 12(5):e0177423. doi.org/10.1371/journal.pone.0177423

Woodruff, D.C. and Fowler, D.W. 2012. Ontogenetic influence on neural spine bifurcation in Diplodo-

coidea (Dinosauria: Sauropoda): a critical phylogenetic character. *Journal of Morphology*, 273:754-764.

Woodruff, D.C. and Fowler, D.W. 2014. The effects of ontogeny in regards to morrison sauropod diversity. Mid-Mesozoic: The age of dinosaurs in transition. *Society of Vertebrate Paleontology 2014 Abstract Volume.*

Woodruff, D.C., Fowler, D.W., and Horner, J.R. 2013. Changes in vertebral morphology associated with histologic data support significant change through ontogeny in diplodocid sauropods. Society of Vertebrate Paleontology 2013 Abstract Volume.

Woodward, H.N., Freedman Fowler, E.A., Farlow, J.O., and Horner, J.R. 2015. *Maiasaura*, a model organism for extinct vertebrate population biology: a statistically robust assessment of growth dynamics and survivorship. *Paleobiology*, 41:503-527.

Woodward, H.N. and Lehman, T.M. 2009. Bone histology and microanatomy of *Alamosaurus sanjuanensis* (Sauropoda: Titanosauria) from the Maastrichtian of Big Bend National Park, Texas. *Journal of Vertebrate Paleontology*, 29:807-821.

APPENDIX 1.

Terms, definition, and usage of pneutmatic morphology and histology used in this analysis.

Pneumatic Architecture (Wedel et al., 2000)

Camera – Round cavity, 5-150 mm in size, septal thickness of 2-10 mm, and a regular branching pattern.

Camella – Angular cavity, 2-20 mm in size, septal thickness of 1-3 mm, and an irregular branching pattern.

Acamerate - Pneumatic structures limited to fossae. Fossae do not significantly invade the centrum.

Procamerate - Deep fossae penetrate to median septum, but are not enclosed by osteal margins.

Camerate - Large, enclosed camerae with regular branching pattern; cameral generations usually limited to 3.

Camellate – Fine internal structures composed entirely of small scaled, thin-walled camellae; can produce a “honeycomb”-like network.

Histologic Terms (Francillon–Vieillot et al., 1990; de Ricqlès et al., 1991; Castanet et al., 1992; Huttenlocker et al., 2013)

Line Of Arrested Growth (LAG) – Thin bands that represent temporary arrest of osteogenesis, and are considered osteological response to predictable environmental cues.

Annuli – Translucent to opaque bands, thicker than LAGs, represent a slowing (but not a cessation) of osteogenesis.

Woven Bone – Highly disorganized arrangement of collagen fibers, which reflects a high rate of osteogenesis.

Fibrolamellar Bone – Woven bone with intervening and randomly oriented primary osteons.

External Fundamental System (EFS) – Slowly deposited parallel-fibered or lamellar tissue along the outermost cortex (closely spaced outermost series of LAGs).

Haversian Bone – Bone that is completely remodeled by secondary osteons.

Primary Osteon – Central blood vessel and surrounding concentric bone tissue.

Secondary Osteon – Osteon formed by replacement of existing bone, surrounded by an outer cement sheath.

Cancellous Bone – Highly vascular bone that contains a higher surface area to mass ratio.

Trabeculae – Rod-shaped bone tissue in cancellous bone. Provides lightweight internal support.

Laminar Vascular Canal – Circumferentially oriented rows of vascular canals.

Longitudinal Vascular Canal – Canals oriented parallel to the long axis on the bone.

Reticular Vascular Canal – Obliquely oriented vascular canals.

APPENDIX 2.

Sauropod specimens examined in this analysis (H-MOS = Histo-Morph Ontogeny Scale [see Appendix 3]).

Specimen Number	Material Examined	Taxonomy	H-MOS Estimation
AMNH 353	Femur	*Apatosaurus* sp. (McIntosh, 1990)	Stage 4
AMNH 435	Femur	*Apatosaurus* sp. (*this analysis*)	Stage 2 or 3
AMNH 606	Femur	*Apatosaurus* sp. (*this analysis*)	Stage 4
AMNH 613	Femur	Diplodocidae (*this analysis*)	Stage 1
AMNH 5855	Femur	*Diplodocus* sp., *Barosaurus* (Mook, 1917; McIntosh, 2005)	Stage 2
AMNH 6341	Vertebrae	*Barosaurus* (Lull, 1919; Tschopp et al., 2015)	Stage 3 or 4
AMNH 7530	Vertebrae	*Barosaurus*, *Kaatedocus* (Michelis, 2004; Tschopp et al., 2015)	Stage 2
AMNH 7535	Vertebrae	*Barosaurus* (Michelis, 2004; Tschopp et al., 2015)	Stage 2 or 3
AMNH 7539	Femur	*Diplodocus* sp. (*this analysis*)	Stage 2
ANS 21122	Vertebrae, Femur, Skull, Dorsal Ribs	*Suuwassea*, Apatosaurinae, Dicraeosauridae (Harris, 2006a,b; Whitlock and Harris, 2010; Woodruff and Fowler, 2012; Tschopp et al., 2015)	Stage 3
BYU 601-17103	Femur	*Apatosaurus* sp. (Wilhite, 2003)	Stage 4
BYU 725-4889	Femur	*Diplodocus* sp. (Wilhite, 2003)	Stage 2
BYU 725-9026	Femur	*Diplodocus* sp. (Wilhite, 2003)	Stage 2 or 3
BYU 725-11421	Femur	*Diplodocus* sp. (Wilhite, 2003)	Stage 2 or 3
BYU 725-12155	Femur	*Diplodocus* sp. (Wilhite, 2003)	Stage 3
BYU 725-13369	Femur	*Diplodocus* sp. (Wilhite, 2003)	Stage 3
BYU 725-13643	Femur	*Diplodocus* sp. (Wilhite, 2003)	Stage 4
BYU 725-13670	Femur	*Diplodocus* sp. (Wilhite, 2003)	Stage 1
BYU 725-16569	Femur	*Diplodocus* sp. (Wilhite, 2003)	Stage 2
BYU 725-16610	Femur	*Diplodocus* sp. (Wilhite, 2003)	Stage 2
BYU 17096	Skull	*Apatosaurus* sp. (Balanoff et al., 2010)	Stage 2
BYU Fe-4-DM197	Femur	*Diplodocus* sp. (Wilhite, 2003)	Stage 3
BYU Fe-5-DM172	Femur	*Diplodocus* sp. (Wilhite, 2003)	Stage 3
CM 84	Vertebrae, Femur	*Diplodocus carnegii* (Hatcher, 1901; Tschopp et al., 2015)	Stage 4
CM 85	Femur	*Apatosaurus* sp. (McIntosh, 1981)	Stage 4
CM 87	Femur	*Apatosaurus* sp. (McIntosh, 1981)	Stage 4
CM 94	Vertebrae, Femur, Dorsal Ribs	*Diplodocus carnegii* (Hatcher, 1901; Tschopp et al., 2015)	Stage 4
CM 555	Vertebrae	*Apatosaurus excelsus*, *Brontosaurus excelsus* (McIntosh, 1981; Tschopp et al., 2015)	Stage 3
CM 563	Vertebrae	*Apatosaurus excelsus*, *Brontosaurus parvus* (Gilmore, 1936; Tschopp et al., 2015)	Stage 4
CM 566	Femur	*Apatosaurus* sp., *Brontosaurus parvus* (McIntosh, 1981; Tschopp et al., 2015)	Stage 1
CM 572	Vertebrae	*Haplocanthosaurus priscus* (Hatcher, 1903; Tschopp et al., 2015)	Stage 3 or 4
CM 879	Vertebrae	*Haplocanthosaurus utterbacki* (Hatcher, 1903; Tschopp et al., 2015)	Stage 2 or 3
CM 3018	Vertebrae, Femur, Skull	*Apatosaurus louisae* (Gilmore, 1936; Tschopp et al., 2015)	Stage 4

Specimen Number	Material Examined	Taxonomy	H-MOS Estimation
CM 3390	Vertebrae	*Apatosaurus* sp. (McIntosh, 1981)	Stage 2
CM 11161	Skull	*Diplodocus longus*; Diplodocinae Indeterminate (Berman and McIntosh, 1978; Tschopp et al. 2015)	Stage 4
CM 11162	Skull	*Apatosaurus louisae* (Berman and McIntosh, 1978; Tschopp et al., 2015)	Stage 4
CM 11338	Vertebrae	*Camarasaurus lentus* (Gilmore, 1925)	Stage 2
CM 21785	Femur	*Apatosaurus* sp. (McIntosh, 1981)	Stage 4
CM 21788	Femur	*Diplodocus* sp. (Wilhite, 2003)	Stage 1 or 2
CM 30762	Femur	*Diplodocus* sp. (Wilhite, 2003)	Stage 2
CM 30766	Femur	*Apatosaurus* sp., Apatosaurine (Wilhite, 2003; Tschopp et al., 2015)	Stage 3
CM 33976	Femur	*Apatosaurus* sp., *Diplodocus* sp. (Wilhite, 2003, *this analysis*)	Stage 1
CM 33991	Femur	*Diplodocus* sp. (McIntosh, 1981)	Stage 1
CMC VP 7747	Femur	Diplodocidae, *Diplodocus* sp. (Meyers, 2004; Woodruff and Fowler, 2004)	Stage 2
CMC VP14128	Skull	*Diplodocus* sp. (this analysis)	Stage 2
CMNH 10039	Femur	*Apatosaurus* sp. (Wilhite, 2003)	Stage 2
CMNH 10380	Vertebrae	*Haplocanthosaurus delfsi* (Wilhite, 2003)	Stage 4
DNM 3781	Femur	*Diplodocus* sp. (Wilhite, 2003)	Stage 4
GPDM 220	Vertebrae	*Camarasaurus* sp. (this analysis)	Stage 4
HMNS 175	Femur	*Diplodocus hayi*, *Galeamopus* (Holland, 1924; Tschopp et al., 2015)	Stage 4
KUVP 1351	Femur	*Apatosaurus* sp. (Wilhite, 2003)	Stage 4
MOR 592	Vertebrae, Femur, Skull, Dorsal Ribs, Cervical Ribs	*Amphicoelias altus*, Dicraeosauridae, *Diplodocus* sp. (Wilson and Smith, 1996; Whitlock and Harris, 2010; Woodruff and Fowler, 2012)	Stage 3
MOR 700 (*2 specimens*)	Skull, Cervical Ribs	*Apatosaurus* sp. (Woodruff and Fowler, 2014)	Stage 2 and 4
MOR 714	Vertebrae	diplodocid indeterminate (this analysis)	Stage 1
MOR 790 (*15 specimens*)	Vertebrae, Femur, Dorsal Ribs, Cervical Ribs	Diplodocinae; *Diplodocus* sp. (Myers, 2004; Woodruff and Fowler, 2012)	Stage 2
MOR 957	Vertebrae, Femur	*Apatosaurus* sp. (*this analysis*)	Stage 4
MOR 7029	Vertebrae, Skull	*Diplodocus* sp. (Woodruff and Fowler, 2014)	Stage 3
MWC 5439	Femur	*Apatosaurus* sp. (this analysis)	Stage 1
MWC “Moffit Co. Apato.”	Femur	*Apatosaurus* sp. (this analysis)	Stage 4
NSMT-PV 20375	Vertebrae, Femur	*Apatosaurus ajax*, Apatosaurinae Indeterminate (Upchurch et al., 2004b; Tschopp et al., 2015)	Stage 4
OMNH 1793	Femur	*Diplodocus* sp. (Wilhite, 2003)	Stage 1
OMNH 01667	Femur	*Apatosaurus* sp. (Wilhite, 2003)	Stage 4
SMA 0003	Vertebrae	Diplodocidae, *Diplodocus* sp. (Schwarz et al., 2007a; *this analysis*)	Stage 3
SMA 0004	Vertebrae, Skull	*Kaatedocus* (Tschopp and Mateus, 2012; Tschopp et al., 2015)	Stage 2 or 3
SMA 0009	Vertebrae, Femur, Cervical Ribs	Diplodocidae; *Barosaurus*, *Brachiosaurus* (Schwarz et al., 2007a; Woodruff and Fowler, 2012; Carballido et al., 2012; Tschopp et al., 2015)	Stage 1
SMA 0011	Vertebrae, Skull	Diplodocidae, *Galeamopus* (Klein and Sander, 2008; Tschopp et al., 2015)	Stage 3

Specimen Number	Material Examined	Taxonomy	H-MOS Estimation
SMA 0014	Femur	Diplodocidae (this analysis)	Stage 4
SMM P84.15.2	Femur	*Apatosaurus* sp. (this analysis)	Stage 1
TMM 993-1	Femur	*Diplodocus* sp. (Wilhite, 2003)	Stage 4
USNM 2672	Skull	*Diplodocus* sp., Diplodocinae Indeterminate (Berman and McIntosh, 1978; Tschopp et al., 2015)	Stage 4
USNM 2673	Skull	*Diplodocus* sp.; *Galeamopus* (Berman and McIntosh, 1978; Tschopp et al., 2015)	Stage 4
USNM 4797	Femur	*Apatosaurus* sp. (Wilhite, 2003)	Stage 4
USNM 10865	Femur	*Diplodocus* sp. (Wilhite, 2003)	Stage 4
USNM 11162	Skull	*Apatosaurus louisae* (Berman and McIntosh, 1978)	Stage 4
USNM 337871	Femur	*Diplodocus* sp. (Wilhite, 2003)	Stage 1 or 2
WDC BS-157	Femur	*Apatosaurus* sp. (Wilhite, 2003)	Stage 3
YPM 429	Vertebrae	Barosaurus (Lull, 1919; McIntosh, 2005; Tschopp et al., 2015)	Stage 4
YPM 1980	Vertebrae	*Apatosaurus excelsus*, *Brontosaurus excelsus* (Ostrom and McIntosh, 1966; Tschopp et al., 2015)	Stage 4
YPM 5862	Femur	*Apatosaurus* sp. (Wilhite, 2003)	Stage 1

APPENDIX 3.

The Histo-Morph Ontogeny Scale (H-MOS).

	Stage 1	Stage 2	Stage 3	Stage 4
HOS	<4	5-7	8-10	>10
Postparietal aperture	?	Present	Present	Absent
LAGs (minimum record via dorsal ribs)	<2	2-6	7 – 15* (15 is an estimated demarcation)	>15
Cervical pneumatic architecture	Acamerate with shallow Fossae (4-8 mm)	Procamerate to Camerate with deepening Fossae (7-24 mm)	Camerate with increasing depth and abundance of Fossae and Foramina	Camerate with extensive and numerous Fossae and Foramina
Cervical pneumaticity (CT scan)	No internal structures	Camerae & Camellae	Thinning median septum with Camerae and Camellae	?
Dorsal pneumaticity (CT scan)	?	Thinning median septum with Camerae	Thinning median septum with Camerae and Camellae	Extensive Camerae in Centrum and Arch
Ant. cervical bifurcation	No bifurcation	No bifurcation	Notched to weakly bifurcated	Fully bifurcated
Post. cervical bifurcation	No bifurcation	Weakly bifurcated	Narrow bifurcation	Fully bifurcated
Ant. dorsal bifurcation	No bifurcation	Narrow bifurcation	Narrow bifurcation	Fully bifurcated
Post. dorsal bifurcation	No bifurcation	Narrow bifurcation	Bifurcated	Fully bifurcated
Ant. Caudal bifurcation	No bifurcation	No bifurcation	No bifurcation	Fully bifurcated
Neural spine Trabeculae (mm)	?	≤ 1	≥ 3	?
Femoral head orientation	?	20° - 11°	10° - 5°	<5°
4th Trochanter position	Proximal	Proximal	Proximal to mid-diaphysis	Mid-diaphysis
Medial Condyle	Not pronounced	Ventrally expanding	Laterally epanding	Greatly pronounced
Femur length (mm)	<800	800 – 1,200	1,200 – 1,450	>1,450
Body mass (kg)	<2,000	2,000 – 3,000	3,000 – 6,000	>6,000

APPENDIX 4.

Diplodocidae body mass table using the allometry based body mass formula of Mazzetta (2004) (log Body Mass = 2.955 x log Femur Circumference − 4.166).

Taxon	Specimen Number	Femur Circumference (mm)	Body Mass (kg)	Mass – Pneumaticity (kg)
Apatosaurus sp.	MWC "Moffat Co. Apato."	908.05	49378.59631	44440.73667
Apatosaurus	SMA 0014	810	26827.06928	24144.36235
Apatosaurus	AMNH 613	805	26340.67055	23706.60349
Apatosaurus	AMNH 606	795	25385.44993	22846.90494
Apatosaurus	AMNH 7539	766	22745.52756	20470.9748
Apatosaurus	AMNH 353	725	19332.98035	17399.68231
A. louisae	CM 30766	701	17502.36514	15752.12863
Brontosaurus	CM 21785	690	16703.17623	15032.8586
Apatosaurus	CM 85	678	15859.29017	14273.36116
Brontosaurus	CM 87	650	14000.9972	12600.89748
Apatosaurus	CM 566	626	12527.86759	11275.08083
Apatosaurus	CM 33976	600	11051.89995	9946.709959
Apatosaurus	P25112	555	8777.801694	7900.021524
Apatosaurus	OMNH 01667	513	6956.5965	6260.93685
Apatosaurus	KUVP 1351	453	4816.928356	4335.235521
Apatosaurus	BS 157	349	2228.687292	2005.818563
Apatosaurus	CMNH 10039	310	1570.26809	1413.241281
Apatosaurus	USNM 4797	288	1263.29507	1136.965563
Apatosaurus	BYU 601-17103	216	539.896901	485.9072109
Apatosaurus	YPM 5862	184.15	336.963175	303.2668575
Apatosaurus	MWC 5439	148	176.6539566	158.9885609
diplodocid indeterminate	SMM P84.15.2	120	95.05622917	85.55060625
Galeamopus	HMNS 175	590	10516.4145	9464.77305
Diplodocus	USMN 10865	564	9205.126313	8284.613681
Diplodocus	TMM 993-1	551	8592.172245	7732.95502
D. carnegii	CM 94	540	8095.12502	7285.612518
Diplodocus	BYU 725-13643	536	7919.211712	7127.290541
Diplodocus	BYU 725-13369	513	6956.5965	6260.93685
D. carnegii	CM 84	510	6837.067544	6153.36079
Diplodocus	BYU Fe-4-DM197	490	6074.764083	5467.287674
Diplodocus	AMNH 435	458	4975.737808	4478.164027
Diplodocus	BYU 725-11421	456	4911.804923	4420.624431
Diplodocus	AMNH 7539	455	4880.043319	4392.038987
Diplodocus	BYU 725-12155	455	4880.043319	4392.038987
Diplodocus	BB 761	451	4754.355816	4278.920235
Diplodocus	BYU Fe-5-DM172	435	4273.028154	3845.725339
Diplodocus	AMNH 5855	410	3587.37103	3228.633927
Diplodocus	MOR 592-35	409	3561.577304	3205.419574
D. longus	CM 30762	387	3024.72504	2722.252536
Diplodocus	BYU 725-16569	385	2978.766464	2680.889817

Taxon	Specimen Number	Femur Circumference (mm)	Body Mass (kg)	Mass – Pneumaticity (kg)
Diplodocus	MOR 790 7-23-95-122	371.5	2680.577713	2412.519942
Diplodocus	BYU 725-16610	365	2544.341575	2289.907418
Diplodocus	MOR 790 7-5-95-7	362	2483.04063	2234.736567
Diplodocus	BB 463	361	2462.826294	2216.543665
Diplodocus	BYU 725-4889	354	2324.36667	2091.930003
Diplodocus	BYU 725-9026	350	2247.610597	2022.849537
Diplodocus	USMN 337871	325	1805.574164	1625.016747
D. longus	CM 21788	317	1677.374822	1509.63734
D. longus	CM 33991	315	1646.295103	1481.665593
Diplodocus	OMNH 1793	254	871.5325918	784.3793326
Diplodocus	DNM 3781	243	764.6567709	688.1910938
Diplodocus	BYU 725-13670	162	230.7368014	207.6631213
diplodocid indeterminate	P.84.15.2	120	95.05622917	85.55060625

APPENDIX 5.

Supplemental Information.

The material contained herein serves to address some of the comments and questions raised by Wedel and Taylor (2013), along with some minor discussion on non-*Apatosaurus* and *Diplodocus* genera.

Anterior Cervical Bifurcation. Wedel and Taylor (2013) suggest that there is no evidence of bifurcated neural spines more anteriorly than C6 in any known North American diplodocid. While it is correct that the anterior most neural spines are damaged and reconstructed from *Diplodocus carnegii* (CM 84), *Brontosaurus excelsus* (YPM 1980), and *Brontosaurus parvus* (UWGM 15556), resulting in unknown spine morphology for these specimens, other cervical series from North American diplodocids do show anterior bifurcation (Appendix 6). The anterior-most cervical neural spines from CM 555 (*Apatosaurus* or *Brontosaurus excelsus*) are damaged, yet C4 distinctly has weak bifurcation. C5 has weakly expressed bifurcation; while C6 and the remaining vertebrae have fully expressed bifurcation. Even within *Barosaurus lentus* we see similar anterior-most bifurcation. In AMNH 7530 (alternatively identified as *Kaatedocus* by Tschopp et al., 2015), the neural spine of C2 is not bifurcated, yet the neural spine of C3 clearly is. After C3, the spines of C4 and C5 are broad, but not bifurcated. The remaining cervical vertebrae are on display, and removal to examine the anterior morphology was not possible at the time of visitation. A slightly larger specimen AMNH 7535 exhibits similar spine morphology. The neural spine of C2 is slightly damaged at the apex, but the neural spine would appear to be bifurcated (if so it would be the anterior most documentation of spine bifurcation). C3 and C5 are missing, and the neural spine of C4 is badly damaged. The neural spine of C6 is clearly bifurcated, yet C7-C13 are un-bifurcated. The final vertebra from this specimen, C14, does have a broad neural spine with incipient or weakly expressed bifurcation.

The claim that no North American diplodocids possessed bifurcated neural spines farther anteriorly than C6 is now shown to be incorrect. Through examination of several complete or nearly complete cervical series, we now see that in diplodocids incipient to weak neural spine bifurcation can occur between C3-C5 (Appendix 6). It is interesting to see that in the anterior most cervical vertebrae there is a small span of bifurcation preceded and followed by a lack of bifurcation. If the hypothesis that bifurcation is developed as a means to maintain and sustain horizontal mobility (Woodruff, 2014) is correct, the presence of select anterior-most bifurcation could be indicative of active cranial mobility. As demonstrated by Wedel and Taylor (2013), serial position is critical. If serial position was unknown in these specimens then there would be a valid argument to place these bifurcated anterior cervicals more posteriorly. From the examined specimens it appears that diplodocids (at least North American taxa) could have neural spine bifurcation prior to C6, and that these damaged historic specimens could be reconstructed with such.

The "End" Of Diplodocid Ontogeny. With the information attained from many of these 2/3 sized diplodocids (such as MOR 592 MOR 7029 [both *Diplodocus* sp.]), it would appear that once a diplodocid reaches roughly 2/3 its maximum length that proportionally (and potentially mechanically) it is more equivalent to the skeletally mature form. Simply applying force per unit area or a Ponderal Index (Thompson, 1942), the gravitational forces acting upon a 15 meter and 27 meter long animal are more similar (approximately 2 times an increase in both body mass and body length) than those acting upon a 2 meter and a 15 meter long animal (approximately 38 times heavier and 7.5 times longer). Once a diplodocid reaches that 2/3 sized threshold it has achieved the skeletal adaptations needed to support the large vertebral column (i.e., bifurcation of the neural spines). From the 2/3 size through the remainder of its life, the animal then modifies the existing structure to deal with the increasing stresses enacted upon it. This explains why the spine bifurcation changes are less dramatic, and why the centrum begins to expand along with other proportional changes. At the point of dramatic weight increase, it is far easier to modify a pre-existing structure than to suddenly develop a new feature. It would appear that from hatching, an immature diplodocid is in a dramatic ontogenetic race to develop the skeletal features needed to support its eventual gigantic girth.

Woodruff and Fowler (2012) Clarification. In the discussion section Woodruff and Fowler (2012) say, "Just as particularly large diplodocid specimens … have been more recently recognized as large and potentially older individuals of already recognized taxa, … taxa defined on small specimens … might represent immature forms of *Diplodocus* or *Apatosaurus*." Clarifying the original

phrasing, the meaning of this passage is that ontogenetic and statigraphic analysis of the characters that diagnose particular taxa within Dipodocoidea (particularly those described based on immature holotypes) may significantly alter the structure of the phylogenetic tree. Further, isolated specimens currently attributed to a given taxon may instead turn out to be ontogenetic stages of a different taxon (without sinking the original designated taxon), these mis-assignments due to heterochronic shifts are only recognizable with stratigraphic and ontogenetic analysis.

Barosaurus. One possible contentious specimen to the ongoing discussion of ontogenetic development of neural spine bifurcation is the immature *Barosaurus* sp. (DINO 2921) described by Melstrom et al. (2016). While documenting numerous important ontogenetic vertebral characters (ranging from Elongation Index, neurocentral fusion, to pneumatic architecture; and thus further verification of the allometric development of the sauropod skeleton), Melstrom et al. (2016) claim that the morphology of the spine bifurcation in this ~1/3 adult sized individual is indistinguishable from that of a mature animal. The precise spinal morphologies and details are hopefully forthcoming (and respectfully such is not demonstrated nor documented in Melstrom et al. [2016]), but perhaps the specimen DINO 2921 could falsify the hypothesis of Woodruff and Fowler (2012).

Yet we would propose that if Melstrom et al. (2016) are indeed correct about the spine morphology of DINO 2921, this could be an incredibly important key to understanding sauropod evolution within the Morrison Formation. If the stratigraphic resolution is correct (see the informative works of K. Truillo), then DINO 2921 comes from the lower portion of the Brushy Basin Member (Turner and Peterson, 1999; Carpenter, 2013), while other immature *Barosaurus* specimens (such as AMNH 7530 and 7535; note Tschopp et al. [2015] identify AMNH 7530 as *Kaatedocus*) are non-bifurcated and come from the upper portion of the Salt Wash Member (Turner and Peterson, 1999; Michelis, 2004; Tschopp and Mateus, 2013). If this resolution, taxonomy, and morphology is correct, then this has substantial implications for *Barosaurus* heterochrony. Again, all of this hinges on the correct initial identification, but if so, this means that Lower and Upper Morrison specimens have differing vertebral biomechanics (i.e., distinct differing morphologies), and given the stratigraphic and calculated temporal range, this may be initial grounds to begin the examination and inquire into heterochrony, and therefore the possibility of two Morrison *Barosaurus* taxa.

Camarasaurus. A minor point we would like to bring to light is the recognition of neural spine bifurcation within the basal macronarian *Camarasaurus*. Woodruff and Fowler (2012) note that in specimens from the Kenton Quarry, the neural spines of immature *Camarasaurus* sp. are morphologically similar to immature diplodocids in that the neural spines are short and non-bifurcated. No in depth examination on *Camarasaurus* sp. was carried out in the preliminary analysis (but is currently underway by DCW), but the possibility of *Camarasaurus* spine ontogeny was favored by Wedel and Taylor (2013). While display features can be modified throughout ontogeny (i.e., male peacock plumage and cassowary and helmeted guinea fowl casques), it would seem unusual that a biomechanical feature could be ontogenetic in one clade, yet static in a closely related clade. In examination of the cervical and dorsal series from the presumed immature *Camarasaurus lentus* (CM 11338), the neural spines are bifurcated, but the depth of bifurcation is shallow and the neural spine apices are much closer together than in a fully mature animal. A relatively small *Camarasaurus* sp. specimen at the Great Plains Dinosaur Museum (GPDM 220) has cervical and dorsal neural spines that likewise exhibit shallow bifurcation and narrow neural spines (Woodruff and Foster, 2017). These features alone have been previously thought to be valid autapomorphies of a new genus (N. Murphy and K. Carpenter, personal commun., 2012). However, analysis by Woodruff and Foster (2017) has contrarily demonstrated that GPDM 220 is a maturationally old, small statured individual. Thus GPDM 220 would further verify the complex relationship between vertebral mechanics and ontogeny within sauropods (Woodruff and Foster, 2017).

Haplocanthosaurus. Wedel and Taylor (2013) perform a laudable job verifying that the genus *Haplocanthosaurus* is not a juvenile *Apatosaurus* or *Diplodocus* (the specific lines of reasoning will not be addressed here but we recommend referral to their text; Wedel and Taylor [2013] p. 23-27). Being one of the rarest of Morrison taxa, *Haplocanthosaurus* is known from three species: *H. delfsi, H. priscus,* and *"H. utterbacki"*. Collected from the lower Brushy Basin Member of the Morrison Formation, CM 572 (*H. priscus*) and CM 879 (*"H. utterbacki"*) both were found meters away from each other in the Marsh-Felch Quarry 1. While CM 879 has not been histologically sampled to assess maturity, the general consensus (largely based on

the overall morphology) is that it represents an immature animal (the differences and validity between *H. priscus* and *H. delfsi* shall not be addressed here; McIntosh and Williams [1988], Wedel and Taylor [2013]). As Wedel (2009) illustrates, CM 572 exhibits widespread neurocentral synostosis, whereas CM 879 exhibits primarily completely unfused neural arches (remember from the manuscript that vertebral fusion is not conclusively indicative of maturity within dinosaurs). Though very weakly expressed and exceedingly rare, incipient neural spine bifurcation has been observed within some specimens of *Haplocanthosaurus* (Appendix 7). Neural spine bifurcation is observed in a posterior dorsal of CM 879, and within an anterior dorsal of CM 572. We are well aware of the importance of serial position and the morphological differences between such vertebrae, however due to the rarity of this feature and the relative proximity a comparison shall still be made. In a posterior cervical of CM 879, the bifurcation is formed by a connection of two closely spaced "humps" (reminiscent of bifurcation observed in CM 555). Within an anterior dorsal of CM 572 these "humps" are spaced and the bifurcation trough is a shallow "V"-shape. Based on the spinal morphology, it would appear that, unlike other members of Diplodocidae, *Haplocanthosaurus* did not biomechanically require neural spine bifurcation. In conjunction with McIntosh and Williams (1988) and Wedel and Taylor (2013), we would consider *"H. utterbacki"* as a *nomen dubium*, and further agree that it represents an immature form of *H. priscus.* In addition to this, the variation between the two specimens would suggest that while incipient, the neural spine bifurcation observed in *Haplocanthosaurus* may also be ontogenetic. Verification of this point requires further specimens and overlapping material.

In regards to the phylogenetic assignment of *Haplocanthosaurus*, we would again stress the need for the recognition of ontogenetic stages. In his analysis of Diplodocoidea, J. Whitlock (2011a) shows that the character matrix for *Haplocanthosaurus* is a combination of several specimens including CM 879 (*"H. utterbacki"*), CM 572 (*H. priscus*), and CMNH 10380 (*H. delfsi*). While these individuals were included to complete otherwise missing characters from other incomplete specimens, the taxonomic uncertainty of *Haplocanthosaurus* could be due to the fact that the characters states representing it are from a combination of varying ontogenetic stages and potentially separate species (*sensu* Mannion et al., 2012).

APPENDIX 6.

Neural spine bifurcation in diplodocid anterior most cervical vertebrae. **1-2,** *Apatosaurus* CM 555; **3,** *Barosaurus* AMNH 7530; **4,** *Diplodocus* sp. MOR 592. B.N.S = Bifurcated Neural Spine. All cervical vertebrae in anterior view. Not to scale. Scale bars equal 10 cm.

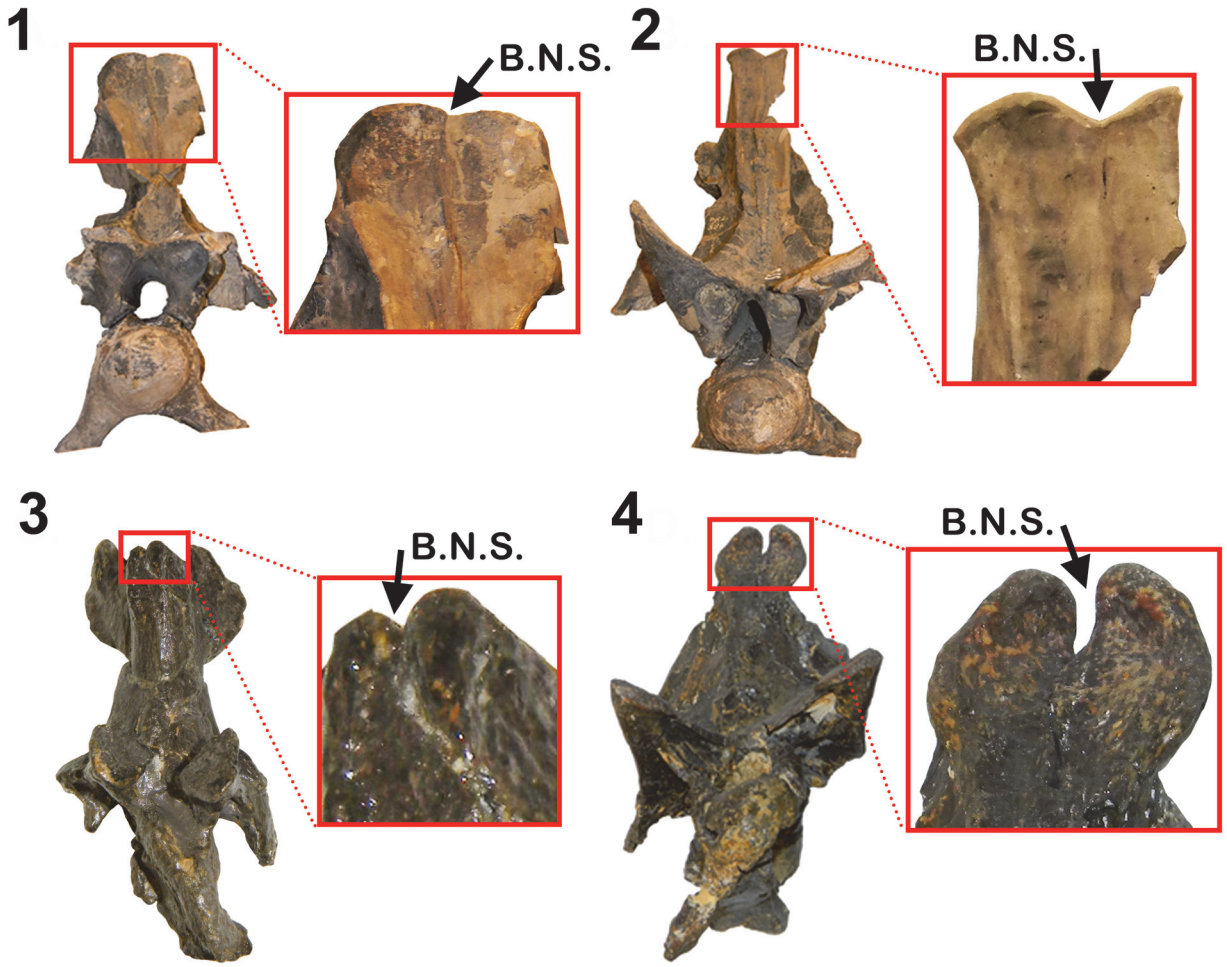

APPENDIX 7.

Haplocanthosaurus incipient neural spine bifurcation. **1,** *Haplocanthosaurus* "*utterbacki*" (CM 879) anterior dorsal in anterior view; **2,** *Hapalocanthosaurus priscus* (CM 529) anterior dorsal in posterior view; **3,** *H.* "*utterbacki*" (CM 879) posterior dorsal in anterior view. I.B. = Incipient Bifurcation. Not to scale. Scale bar equals 10 cm.

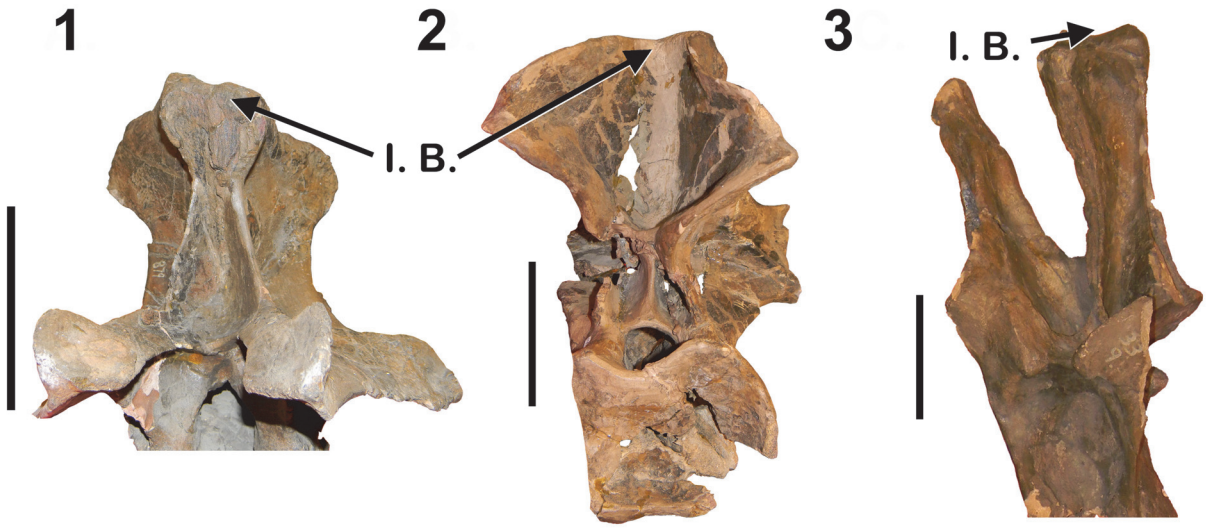

APPENDIX 8.

Elongation Index of diplodocid cervical vertebrae (EI = centrum length divided by cotyle diameter).

Diplodocus

HQ 1 SMA 0003

	Centrum Length (mm)	Cotyle Diameter (mm)	EI
C2	84	37	2.27027
C3	105.5	31	3.40323
C4	131	46.5	2.8172
C5	184	30.5	6.03279
C6	228	46	4.95652
C7	280	44	6.36364
C8	376	55.5	6.77477
C9	375	71	5.28169
C10	385	49	7.85714
C11	431	75	5.74667
C12	458	74	6.18919
C13	454	58.5	7.76068
C14	463	77	6.01299
C15	474	77	6.15584

HQ 2 SMA 0004

	Centrum Length (mm)	Cotyle Diameter (mm)	EI
C2	83.5	35	2.38571
C3	107	27	3.96296
C4	132	-	-
C5	158	28	5.64286
C6	192	26.5	7.24528
C7	218	37	5.89189
C8	247	34.5	7.15942
C9	264	38	6.94737
C10	296	53	5.58491
C11	295	51	5.78431
C12	316	56	5.64286
C13	326	66	4.93939
C14	314	61	5.14754

MOR 592

	Centrum Length (mm)	Cotyle Diameter (mm)	EI
C2	114.4	41.2	2.7767

C3	128.3	41.9	3.06205
C4	-	-	-
C5	163.6	49	3.33878
C6	-	-	-
C7	247	37.5	6.58667
C8	256.5	47.4	5.41139
C9	271.6	67.8	4.0059
C10	291	62.4	4.66346
C11	279.4	103.5	2.69952
C12	266.7	112.5	2.37067
C13	239.2	180.8	1.32301
C14	349.3	73.2	4.77186
C15	304.8	96.2	3.1684

CM 84

	Centrum Length (mm)	Cotyle Diameter (mm)	EI
C2	165	54	3.05556
C3	243	69	3.52174
C4	289	81	3.5679
C5	372	94	3.95745
C6	442	99	4.46465
C7	485	114	4.25439
C8	512	120	4.26667
C9	525	159	3.30189
C10	595	175	3.4
C11	605	210	2.88095
C12	627	225	2.78667
C13	638	231	2.7619
C14	642	295	2.17627
C15	595	245	2.42857

Apatosaurus

CM 555

	Centrum Length (mm)	Cotyle Diameter (mm)	EI
C2	140	63	2.22222
C3	221	84	2.63095
C4	274	96	2.85417
C5	270	60	4.5

C6	295	114	2.58772
C7	316	-	-
C8	344	113	3.04425
C9	380	-	-
C10	-	-	-
C11	480	193	2.48705
C12	460	245	1.87755
C13	-	-	-
C14	378	260	1.45385
C15	-	-	-

CM 563

	Centrum Length (mm)	Cotyle Diameter (mm)	EI
C3	250	80	3.125
C4	300	125	2.4
C5	342	134	2.55224
C6	-	-	-
C7	415	170	2.44118
C8	415	205	2.02439
C9	445	215	2.06977
C10	475	250	1.9

NSMT-PV 20375

	Centrum Length (mm)	Cotyle Diameter (mm)	EI
C3	352	97	3.62887
C4	-	-	-
C5	375	155	2.41935
C6	395	195	2.02564
C7	420	220	1.90909
C8	395	195	2.02564
C9	380	235	1.61702
C10	390	-	-
C11	-	-	-
C12	475	240	1.97917
C13	-	-	-
C14	450	305	1.47541

CM 3018

	Centrum Length (mm)	Cotyle Diameter (mm)	EI
C2	190	85	2.23529
C3	280	100	2.8
C4	370	100	3.7
C5	-	-	-

C6	440	150	2.93333
C7	450	190	2.36842
C8	485	225	2.15556
C9	510	230	2.21739
C10	530	250	2.12
C11	550	240	2.29167
C12	490	265	1.84906
C13	480	-	-

Barosaurus

AMNH 7530

	Centrum Length (mm)	**Cotyle Diameter (mm)**	**EI**
C2	80	14	5.71429
C3	75	26	2.88462
C4	97	37	2.62162
C5	123	62	1.98387

C6-C12 are on display and could not be measured first hand

AMNH 7535

	Centrum Length (mm)	**Cotyle Diameter (mm)**	**EI**
C2	87	15	5.8
C3	-	-	-
C4	102.5	23	4.45652
C5	-	-	-
C6	135	25	5.4
C7	140	21	6.66667
C8	166	36	4.61111
C9	-	-	-
C10	-	-	-
C11	234	32	7.3125
C12	-	-	-
C13	281	30	9.36667
C14	323	47	6.87234

AMNH 6341 (from McIntosh, 2005)

	Centrum Length (mm)	**Cotyle Diameter (mm)**	**EI**
C8	618	130	4.75385
C9	685	123	5.56911
C10	737	168	4.3869
C11	775	145	5.34483
C12	813	155	5.24516
C13	850	180	4.72222

C14	865	155	5.58065
C15	840	160	5.25
C16	750	250	3

YPM 429 (from McIntosh, 2005)

	Centrum Length (mm)	Cotyle Diameter (mm)	EI
C13	930	220	4.22727
C14	890	345	2.57971
C15	-	300	-
C16	720	365	1.9726